

Comparison Between PBE-D3, B3LYP, B3LYP-D3 and MP2 Methods for Quantum Mechanical Calculations of Polarizability and IR-NMR Spectra in C₂₄ Isomers, Including a Novel Isomer with D_{2d} Symmetry

Futtaim Alhanzal^{a,*,d}, Nabil Joudieh^{a,*,d}, Khansaa Hussein^{c,*,d}, and Nidal Chamoun^{b,*,d}

^a Faculty of sciences, Physics Department, Damascus University, P.O. Box 30621, Damascus, Syria.

^b Physics Department, HIAST, P.O. Box 31983, Damascus, Syria .

^c Faculty of sciences, Chemistry Department, Damascus University, P.O. Box 30621, Damascus, Syria.

* Correspondence: fattomm90@gmail.com ; futtaim91.alhandel@damascusuniversity.edu.sy ; njoudieh@yahoo.fr ; khansaa1.hussein@damascusuniversity.edu.sy; nidal.chamoun@hiast.edu.sy.

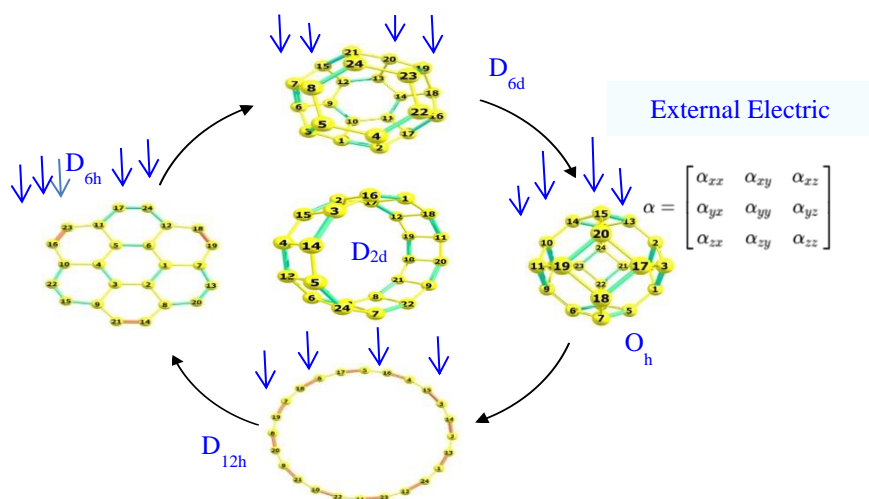
^d These authors contributed equally to this work.

Abstract

In this study, we performed a comprehensive theoretical analysis of C₂₄ isomers in the gaseous phase using the PBE-D3/cc-pVTZ, B3LYP/cc-pVTZ, B3LYP-D3/cc-pVTZ and MP2/6-31G methods. We also considered the basis set cc-pVTZ for the MP2 method, and carried out optimized (single point) calculations in three (remaining two, where convergence was too much time consuming) isomers in order to reveal the potentiality of the method. Our investigation covered a wide range of properties, including geometry optimizations, chemical stability, polarizabilities, nuclear screening constants, Fermi (FE), gap (GE), and atomization energies (AE), thermodynamic analysis, reactivity index, as well as IR and NMR spectra. These calculations were performed for the ring (D_{12h}), sheet (D_{6h}) and two cage (D_{6d} and O_h) configurations. Interestingly, we also proposed a new structure, the bracelet (D_{2d}) arrangement, which appeared to be stable according to the PBE, B3LYP and B3LYP-D3 methods, but was classified as a transition state by the MP2 method. The results consistently indicated that the D_{6h} isomer is the most stable one among the C₂₄ isomers studied, while the D_{2d} isomer was found to be the least stable. Regarding the gap energy (GE), the B3LYP and B3LYP-D3 methods consistently yielded higher values compared to the PBE's, with an average DFT (PBE and B3LYP) GE of 1.89 eV, whereas the MP2 method showed a substantially higher GE value of 7.6 eV, representing an increase of approximately 75%. Additionally, the polarizabilities of the C₂₄ isomers were found to be overestimated by the PBE, B3LYP, and B3LYP-D3 methods when compared to the corresponding MP2 values. The PBE-D3 method consistently produces higher polarizabilities for the C₂₄ isomers in comparison to B3LYP, B3LYP-D3, and MP2 methods. The investigation confirms that the O_h (D_{12h}) isomer has the smallest (largest) polarizability, as agreed upon by all methods. Moreover, the polarizability of D_{12h} is notably affected by the selected DFT method, while that of O_h displays lower sensitivity but shares similarities with D_{6d}. However, for the newly proposed D_{2d} isomer, the

polarizability is ranked third (fourth) in ascending order with the PBE-D3 (B3LYP-D3) method. This highlights the importance of considering the electronic correlation and dispersion effects in accurately predicting polarizabilities. The results obtained from different methods shed light on the impact of methodology choice on the predicted properties, emphasizing the need for careful consideration when analyzing and interpreting theoretical results for such various geometries.

Graphical Abstract



Keywords: C₂₄ isomers, Polarizability, Spectra, PBE-D3 method, B3LYP method, MP2 method.

Contents

1. Introduction.....	3
2. Computational Methods.....	5
3. C ₂₄ Isomers: Quantum Mechanical Characterization and Properties.....	5
3.1. Geometry optimizations of C ₂₄ isomers.....	5
3.2. Stability, Gap, Fermi and Atomization energies.....	10
3.3. Electronic Properties of C ₂₄ Isomers: Ionization potential, Electronic Affinity, Hardness and Electronegativity.....	16
3.4. Electric dipole moment and Polarizabilities.....	19
3.5. Vibration frequencies and infrared spectra.....	23
3.6. NMR spectra for the C ₂₄ isomers.....	25
4. Conclusion.....	27
Declaration of competing interest.....	28
Acknowledgments.....	28
Supporting Information Available.....	28
References.....	28

1. Introduction

Fullerenes, which were discovered in the late eighties [1], are a fascinating form of carbon, known as its third allotropic form. Fullerenes consist of sp^2 hybridized carbon atoms bonded together in the form of a hollow sphere with different sizes such as C_{20} , C_{24} , C_{60} , etc. [2]. Among the various fullerenes, C_{20} is the most recently discovered one [3]. Subsequently, medium and large sizes of fullerenes molecules were discovered, with some reaching up to 6000 carbon atoms [4]. Following the discovery of the C_{60} fullerene in 1985 [5], numerous theoretical and experimental studies have been conducted aiming at investigating the structures and stability of small fullerenes containing fewer than 60 carbon atoms, by using the mass spectrometry methods [6-16]. The C_{24} fullerene, one of the smallest fullerenes, was first reported in 1993 [17] and produced, under certain experimental conditions, from carbon vapor condensation. It has four isomers, namely the ring, sheet, and cages (fullerene-like), but the most common is the D_{6d} cage isomer which contains two hexagons with 12 pentagons between them [6,18,19]. At the theoretical level, Jensen and Toftlund [20] investigated the four isomers of C_{24} fullerene: cages (D_{6d} , O_h), ring (D_{12h}), and sheet (D_{6h}) using the Hartree-Fock (HF) method and second-order Moller-Plesset perturbation theory (MP2) with a DZP basis set. Their study showed that the D_{6h} sheet isomer is the most stable, followed by the D_{6d} cage isomer. In 1998 [21], the energy difference between the ring and fullerene forms of C_{24} has been calculated using ab initio methods, which were compared to density functional methods. The calculations strongly suggest that the fullerene form is favored by 80 kcal/mol over a monocyclic ring structure. In 1997, Balevišius *et al.* [22] studied the chemical stability and electronic properties of the D_{6d} isomer using the PM3 method implemented in the MOPCA program [23]. In 2007, the geometrical parameters, total energy, heat of formation, energies of HOMO and LUMO orbitals, and density of one electron states (DOS) were determined by using semi-empirical quantum chemistry PM3 method for cubic polymerized structures of the O_h isomer [24]. The results of calculations allow for the existence of a polymerized cubic crystal structure based on all the considered small fullerenes. In 2012, Anafche and Naderi [25] reported results concerning the structural stabilities, geometry, electronic properties, and binding energies of $C_{24}(D_{6d})$ and some of its hetero fullerene derivatives at the B3LYP/6-311-EFG**//B3LYP/6-31+G* level of theory. Recently, several studies [26-28] focused on the C_{24} fullerene and its four isomers by studying their geometry, energy stability, spectra, and interactions with other molecules. Using density functional theory (DFT) and coupled cluster calculations, the relative energies and infrared spectra have been determined for the four different types of C_{24} isomers. Among the four isomers, it was found that the graphene (sheet) form of C_{24} best accommodates astronomical data [28]. Recent research activities in various fields including molecular electronics, molecular devices, nanometer electronics, nanotechnology, energy storage, and biomedical/nanomedicine applications, demonstrate that fullerene C_{24} is becoming increasingly connected to several nano themes. As a carbon material, the C_{24} isomer is considered a promising candidate for future developments in nanotechnology, for both civil and military/ defense applications. Studies have demonstrated its potential in fields such as superconductivity

and electronic transport properties, highlighting its applicability in nanometer electronics. The importance of C_{24} is also seen in its hydrogen storage capabilities, an important consideration in the energetic domain [29,30]. An important view on these directions is the work of Sawhney et al. [29] regarding the superconductive properties of C_{24} and its doped counterparts. Their results clearly exhibited the better electrical performance of the pure C_{24} over its doped counterparts for cryogenic electronic applications. As to single molecular devices and nanometer electronics, we report the work of When-Kai Zhao et al. [30], which studied the orientation effect on the electronic transport properties of C_{24} fullerene between the electrodes (Au- C_{24} -Au). These results confirm the applicability potential and importance of C_{24} fullerene in nanometer electronics. The energy storage domain constitutes another important application. Actually, the hydrogen storage capability in fullerene constitutes an increasingly significant area of interest, and the hydrogen storage properties of C_{24} fullerene were studied using the DFT recently [31-33], where this capacity was found to approximate 10-12 wt. %. Also, Mahamiya et al. [34] conducted a theoretical study on the hydrogen storage capacity of yttrium atom-decorated C_{24} fullerene. Their results show that a single yttrium atom attached to C_{24} fullerene can reversibly adsorb a maximum number of 6 H_2 molecules. Using the DFT, Mahamiya et al. [35] showed in 2022, that the scandium-decorated C_{24} fullerene can adsorb up to six hydrogen molecules with an average adsorption energy of -0.35 eV per H_2 and an average desorption temperature of 451 K, and also demonstrated that the scandium-decorated C_{24} fullerene system is thermodynamically stable, providing thus a potential promising candidate for a reversible high-capacity hydrogen storage device.

In this study, we focus on the C_{24} fullerene and its importance in various fields such as technology and nano-science. Since there is relatively limited theoretical research on C_{24} , we aim to bring a contribution by examining its isomers. In our investigation, based on the study conducted by Zhang and Dolg [36], we have introduced a novel structure called the "bracelet" with D_{2d} symmetry and thoroughly examined its stability using computational methods. To assess stability, we employed the PBE-D3, B3LYP and B3LYP-D3 methods with the cc-pVTZ basis set and the MP2 method with two basis sets 6-31G and cc-pVTZ. By calculating the IR spectra frequencies, we were able to confirm the stability of the bracelet structure using the PBE-D3, B3LYP and B3LYP-D3 methods with the cc-pVTZ basis set. However, when we applied the Møller-Plesset second-order perturbation theory (MP2/6-31G), we encountered a discrepancy indicating that the structure may exhibit characteristics of a transition state. This inconsistency is likely due to the utilization of a non-extended basis set (6-31G) during the optimization process for the MP2 calculations, and to the fact that the latter method in itself does not take the dispersion interactions into consideration, in contrast to the PBE method which accounts explicitly for the dispersion, and the B3LYP which does this implicitly through suitable parametrization.

Unsatisfactorily, the MP2/cc-pVTZ optimization for the D_{2d} (Bracelet) and D_{6d} (Cage) isomers did not converge, even after an unusually long computation time. The fact that the optimization did converge for the O_h (cage), the D_{6h} (sheet), and the D_{12h} (ring) isomers suggests that the structural arrangement in a cage (bracelet) for D_{6d} (D_{2d}) may not be the primary cause of the convergence issue. It is possible that the intrinsic

structure of the potential energy hypersurface, combined with the nature of the MP2 method and the size of the basis set, is the underlying reason for the convergence problem. In order to qualitatively assess the impact of extending the basis set from 6-31G to cc-pVTZ using the MP2 method, a single MP2/cc-pVTZ point calculation was performed for the studied isomers.

Furthermore, we conducted a comprehensive quantum mechanical analysis on classical fullerenes and nonfullerene isomers. This analysis encompassed the use of various computational methods, including PBE-D3, B3LYP, B3LYP-D3 and MP2, implemented through the ORCA 5.0.1 program package. We thoroughly investigated several properties such as static electric polarizabilities, NMR and IR spectra, energy quantities (including gap, Fermi, and atomization energies), as well as thermodynamic properties. The results obtained were meticulously examined and presented in the study.

2. Computational Methods

The computational calculations were carried out using the ORCA 5.0.1 program package [37]. Four distinct levels of calculations were employed: PBE-D3, B3LYP, B3LYP-D3 with the cc-pVTZ basis set, and MP2/6-31G. For the PBE-D3, B3LYP and B3LYP-D3 calculations, the optimization of molecular geometry was performed along with the determination of energetic properties, static electric Polarizabilities, dipole moment, and the computation of IR frequencies as well as IR and NMR spectra. The same perturbation order in MP2/6-31G was utilized to calculate these parameters. An optimized (single) energy calculation using MP2/6-31G (MP2/cc-pVTZ) was also carried out. Chemcraft [38], a graphical interface for drawing, was used in conjunction with the ChemDraw feature to obtain the visual representations of the five shapes and to generate the corresponding IR and NMR spectra.

3. C₂₄ Isomers: Quantum Mechanical Characterization and Properties

A comprehensive quantum mechanical analysis was conducted to characterize the structures and properties of the five C₂₄ isomers (D_{6d}, O_h, D_{12h}, D_{6h}, and D_{2d}) using four distinct levels of theory. The analysis encompassed tasks such as geometry optimization, evaluation of chemical stability, calculation of polarizabilities and various energy parameters, determination of vibration frequencies, and theoretical predictions of both infrared and NMR spectra for each isomer at all four levels of theory, whereas the optimized energies and thermodynamic properties of the isomers under study are reported in Tables S1 and S2 of the supporting information file.

3.1. Geometry optimizations of C₂₄ isomers

Table 1 to 5 present the optimized key bond lengths and angles obtained from calculations using the PBE-D3/cc-pVTZ, B3LYP/cc-pVTZ, B3LYP-D3/cc-pVTZ and MP2/6-31G methods for the five C₂₄ isomers, and from the MP2/cc-pVTZ method for the D_{12h}, D_{6h} and O_h isomers.

Bond lengths are denoted as r (in Angstroms), while the angles are denoted as A (in degrees). The optimized geometries of the five C_{24} isomers are depicted in Figure 1. The D_{6d} cage structure consists of one hexagonal ring at the top and bottom, with 12 pentagonal rings in the middle. A total of 36 C-C bonds in the D_{6d} structure are classified into four categories, whereas in the O_h cage structure these bonds alternate between single and double character. The optimized bond lengths are in good agreement with previously reported values of 1.38 Å and 1.50 Å [39]. The sheet isomer D_{6h} comprises interconnected hexagonal polygons, while the ring isomer D_{12h} features a circular arrangement of carbon atoms. The newly proposed D_{2d} isomer consists of two rings connected by single bonds, along with 12 quadrilateral polygons in the middle. Figure 1 illustrates the optimized structures obtained using the PBE-D3/cc-pVTZ method for the C_{24} isomers.

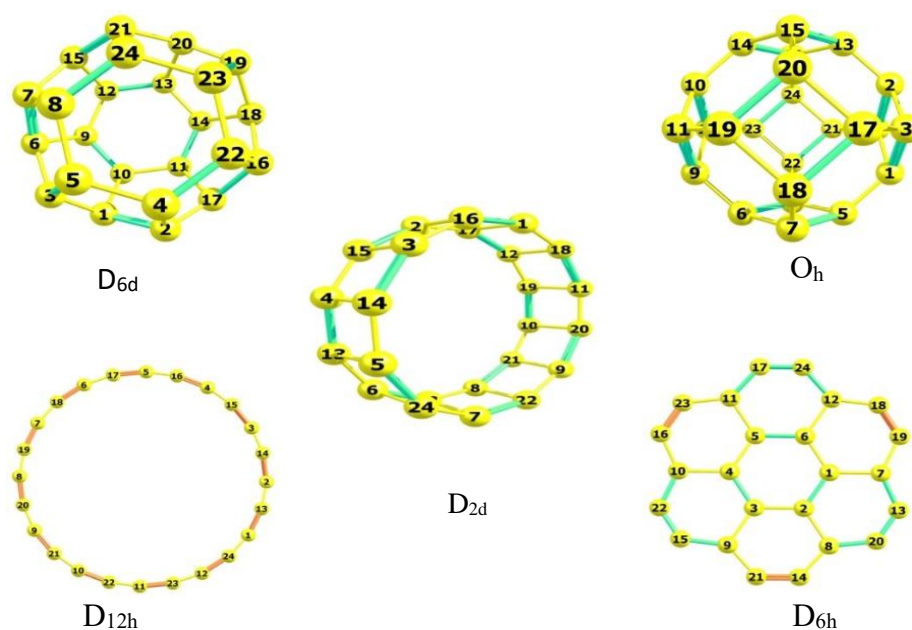


Fig.1. Optimized PBE-D3/cc-pVTZ geometry of the five C_{24} isomers.

Table 1. Bond lengths (r in Angstrom) and angles' measurements (A in degrees) at PBE-D3/cc-pVTZ, B3LYP/cc-pVTZ, B3LYP-D3/cc-pVTZ, MP2/cc-pVTZ and MP2/6-31G levels for the D_{6d} Cage.

Isomer	D_{6d} Cage						
	cc-pVTZ				6-31G	B3LYP/ 6-31G(d) [27]	MP2/DH(d) [21]
Method	PBE-D3	B3LYP	B3LYP-D3	MP2	MP2		
$r(19-18)$	1.465	1.458	1.462	-	1.405	1.398	1.365
$r(19-20)$	1.428	1.358	1.360	-	1.476	1.457	1.463
$r(19-23)$	1.443	1.529	1.535	-	1.556	1.523	1.531
$r(22-23)$	1.465	1.417	1.418	-	1.450	1.437	1.423
$r(10-11)$	1.409	-	-	-	-	-	-
$r(21-24)$	1.528	-	-	-	-	-	-
$r(22-16)$	1.512	-	-	-	-	-	-

A(2-1-10)	106.58	107.34	107.19	-	108.93	-	-
A(2-1-3)	108.85	109.10	109.22	-	109.11	-	-
A(6-3-5)	105.87	107.30	107.16	-	-	-	-
A(5-4-22)	118.19	119.94	119.94	-	119.99	-	-
A(6-9-10)	108.37	106.05	106.12	-	-	-	-
A(9-10-11)	119.19	120.00	120.01	-	-	-	-
A(1-3-5)	109.86	-	-	-	107.55	-	-
A(1-3-6)	112.70	-	-	-	-	-	-
A(3-1-10)	103.16	-	-	-	107.56	-	-
A(2-4-22)	107.39	-	-	-	106.25	-	-
A(4-5-8)	122.61	-	-	-	120.00	-	-
A(1-2-17)	110.24	-	-	-	-	-	-

Table 2. Bond lengths (r in Angstrom) and angles' measurements (A in degrees) at PBE-D3/cc-pVTZ, B3LYP/cc-pVTZ, B3LYP-D3/cc-pVTZ, MP2/cc-pVTZ and MP2/6-31G levels for the O_h Cage.

Isomer	O _h Cage						
	Basis set	cc-pVTZ				6-31G	B3LYP/ 6-31G(d) [27]
Methods	PBE-D3	B3LYP	B3LYP-D3	MP2	MP2		
r(2,3)	1.494	1.489	1.494	1.483	1.520	1.457	1.463
r(2,13)	1.378	1.368	1.368	1.387	1.402	1.398	1.365
A(20-17-18)	90.00	90.00	90.00	90.00	90.00	-	-
A(13-2-3)	120.00	120.00	120.00	120.00	120.00	-	-

Tables 1 and 2 provide the bond lengths and angles for the D_{6d} and O_h cage at the PBE-D3/cc-pVTZ, B3LYP/cc-pVTZ, B3LYP-D3/cc-pVTZ, and MP2/6-31G levels. The D_{6d} cage exhibits four types of carbon-carbon bond lengths at the MP2/6-31G level, with an average length of 1.477 Å. In contrast, the O_h isomer shows two types of bond lengths across all four methods, including the MP2 method in two different basis sets. The B3LYP/cc-pVTZ and PBE-D3/cc-pVTZ methods yield similar results, with an increase in bond types observed for the D_{6d} cage in the PBE-D3/cc-pVTZ calculations, resulting in an average bond length of 1.447 Å. This increase can be attributed to the incorporation of dispersion terms in the PBE-D3 method. These findings are consistent with a previous study [19], which reported bond lengths of 1.423, 1.531, 1.462 Å, and 1.369 Å for the optimized D_{6d} structure. For the O_h isomer, the carbon-carbon bond lengths were determined to be 1.3782 and 1.4957 Å at the B3LYP/cc-pVDZ level, in agreement with the MP2/6-31G calculations [19]. Regarding the angle measurements, the D_{6d} isomer exhibits angles ranging from 106.7° to 120.0°, while the O_h isomer displays angles within the range of 119.9° to 89.9°. The angles within the pentagons of both cage isomers deviate slightly from the ideal value of 108° for a regular pentagon. However, the angles within the hexagonal polygons closely approximate the expected value of 120° for a regular hexagon. For instance, at the PBE-D3 level, the angle A

(1,2,10) of the D_{6d} isomer measures 106.58° , which is 1.58° less than the regular pentagon angle, while the A(1,3,5) angle measures 109.86° , exceeding the regular pentagon angle by 1.86° . The angles within the quadrilaterals and hexagons of the O_h isomer are nearly equal to the expected values of 120° and 90° , respectively. Furthermore, by examining the results in Tables 1 and 2, it can be observed that the empirically corrected dispersion terms (B3LYP-D3) have minimal impact on the B3LYP geometry.

Table 3. Bond lengths (r in Angstrom) and angles' measurements (A in degrees) at PBE-D3/cc-pVTZ, B3LYP/cc-pVTZ, B3LYP-D3/cc-pVTZ, MP2/cc-pVTZ and MP2/6-31G levels for the Ring D_{12h} .

Isomer	D_{12h} Ring						
	cc-pVTZ				6-31G	HF/DZP [20]	MP2/DH(d) [21]
Methods	PBE-D3	B3LYP	B3LYP-D3	MP2	MP2		
r(16-4)	1.327	1.336	1.335	Unstable	Unstable	1.385	1.345
r(4-15)	1.248	1.228	1.227			1.197	1.266
A(4-15-3)	165.01	164.95	164.95	-	-	-	165.00
A(3-14-2)	164.99	165.06	165.06			-	-

Table 4. Bond lengths (r in Angstrom) and angles' measurements (A in degrees) at PBE-D3/cc-pVTZ, B3LYP/cc-pVTZ, B3LYP-D3/cc-pVTZ, MP2/cc-pVTZ and MP2/6-31G levels for the Sheet D_{6h} .

Isomer	D_{6h} Sheet						
	cc-pVTZ				6-31G	HF/DZP [20]	B3LYP/cc-pVDZ [19]
Methods	PBE-D3	B3LYP	B3LYP-D3	MP2	MP2		
r(1-2)	1.444	1.442	1.441	1.443	1.466	1.391	1.391
r(6-12)	1.496	1.483	1.482	1.485	1.495	1.456	1.488
r(12-24)	1.385	1.383	1.383	1.384	1.409	1.447	1.450
r(17-24)	1.241	1.228	1.228	1.254	1.275	1.210	1.240
A(6-1-2)	120.00	120.01	120.01	120.00	119.82	112.60	-
A(1-2-3)	119.99	119.99	119.99	120.00	119.82	127.40	-
A(6-12-24)	112.13	112.13	112.17	112.76	113.19	120.00	-
A(10-16-23)	127.86	127.86	127.82	127.23	126.69	-	-

Tables 3 and 4 present the bond lengths and angles for the D_{12h} (Ring) and D_{6h} (Sheet) isomers at the PBE-D3/cc-pVTZ, B3LYP/cc-pVTZ, B3LYP-D3/cc-pVTZ, MP2/cc-pVTZ and MP2/6-31G levels. The ring isomer D_{12h} exhibits two types of bond lengths at the PBE-D3, B3LYP and B3LYP-D3 levels, while it is unstable at both the optimized MP2 levels, with either 6-31G or cc-pVTZ basis set. On the other hand, the sheet isomer D_{6h} displays four different types of bonds across all four methods, where the calculations of the MP2 method were done for two different basis sets. The angles in the D_{12h} isomer fall within the range of 164.9° to 165.0° , while the angles in the D_{6h} isomer range from 112.28° to 127.71° . These angle values deviate slightly from those of a regular hexagon, which is consistent with previous studies [19,20,21]. Furthermore,

when comparing the results of B3LYP-D3 and B3LYP for both D_{12h} and D_{6h} isomers, it can be observed that the dispersion correction only introduces minor changes. However, when we compare the optimized results of MP2/6-31G and MP2/cc-pVTZ, we find that the differences are small but significant, clearly distinguishing between the two types of calculations. It is worth noting that transitioning from the 6-31G basis set to the cc-pVTZ basis set has the effect of reducing the values of bond lengths and angles. Moreover, it is noteworthy that the results obtained with MP2/cc-pVTZ are very close to those of PBE and B3LYP-D3, with the exception of the value of r (17-24).

Table 5 provides the bond lengths and angle measurements for the D_{2d} isomer at the PBE-D3/cc-pVTZ, B3LYP/cc-pVTZ, B3LYP-D3/cc-pVTZ and MP2/6-31G levels. The D_{2d} isomer exhibits three types of bond lengths with an average length of 1.470 Å at the PBE-D3/cc-pVTZ level of computation, being slightly reduced to 1.465 Å at the B3LYP/cc-pVTZ level, whereas the B3LYP-D3/cc-pVTZ level yields the shortest average bond length of 1.462 Å, showing that the dispersion correction introduced by B3LYP-D3 causes only minor modifications. The angles in this isomer range from 88° to 150°. However, at the MP2 level, the D_{2d} isomer is in a transitional state with a negative frequency of -313.33 cm^{-1} . While the B3LYP/cc-pVTZ method used in our study does not explicitly consider dispersion interactions, it is still considered a reliable functional for studying various molecular systems. Indeed, the B3LYP-D3 geometry is similar and nearly identical to that of B3LYP, which reduces the impact of the dispersion correction on the D_{2d} structure. The negligible influence due to dispersion results in similar results of both B3LYP and B3LYP-D3 regarding energy and electrical properties. This finding suggests that the PBE-D3 method used in our analysis not only uses a reliable functional but also effectively incorporates dispersion forces and is specifically designed to accurately capture non-covalent interactions in molecular structures. Although there is limited experimental data available for the C_{24} isomers, we recommend the use of the PBE-D3 method, which is particularly well-suited for investigating systems where dispersion and long-range interactions play a crucial role, such as the isomers under study. Therefore, the stability prediction of the D_{2d} and D_{12h} isomers by the PBE-D3 method, which takes into account dispersion interactions and non-covalent interactions, provides further support for its potential stability compared to the instability observed in the MP2 method.

Table 5. Bond lengths (r in Angstrom) and angles' measurements (A in degrees) at PBE-D3/cc-pVTZ, B3LYP/cc-pVTZ, B3LYP-D3/cc-pVTZ and MP2/6-31G levels for the D_{2d} isomer (TS means "Transition State").

Isomer	D_{2d} Bracelet			
Basis set	cc-pVTZ			6-31G
Method	PBE-D3	B3LYP	B3LYP-D3	MP2
$r(4-13)$	1.482	1.483	1.478	-
$r(13-6)$	1.393	1.379	1.380	-
$r(13-5)$	1.525	1.517	1.527	-
$A(4-13-6)$	150.01	150.03	150.02	-
$A(6-23-8)$	149.95	149.88	149.92	-
$A(24-6-13)$	91.67	91.97	91.85	-

A(13-5-24)	88.33	88.02	88.14	-	
------------	-------	-------	-------	---	--

The average values of single, double, and triple bond lengths in the studied isomers are reported in Table 6. Upon examination of this table, it can be observed that for the D_{6d} , D_{2d} , and D_{12h} isomers, the PBE-D3 method yields result that are nearly equivalent to those obtained with the B3LYP and B3LYP-D3 methods, while the MP2 method slightly overestimates the bond lengths compared to the previous three methods. In the case of the D_{6h} isomer, both the PBE-D3 and B3LYP methods show almost identical results, while the MP2 method underestimates the bond lengths when compared to them. For the two isomers, O_h and D_{6h} , both MP2/6-31G and MP2/cc-pVTZ methods yield average bond lengths of similar orders of magnitude but with significantly different values. This clearly demonstrates the impact of expanding the basis set.

Table 6. The average values of the simple and multiple bond lengths at PBE-D3/cc-pVTZ, B3LYP/cc-pVTZ, B3LYP-D3/cc-pVTZ, MP2/cc-pVTZ and MP2/6-31G levels for C_{24} isomers.

Basis set	Method	Distance	D_{6d}	O_h	D_{12h}	D_{6h}	D_{2d}
cc-pVTZ	PBE-D3	\bar{r}_{C-C}	1.466	1.436	1.247	1.440	1.459
		$\bar{r}_{C=C}$	1.428	1.494	-	1.363	1.482
		$\bar{r}_{C\equiv C}$	-	-	1.327	1.241	-
	B3LYP	\bar{r}_{C-C}	1.458	1.458	1.228	1.434	1.448
		$\bar{r}_{C=C}$	1.434	1.489	-	1.359	1.483
		$\bar{r}_{C\equiv C}$	-	-	1.336	1.228	-
	B3LYP-D3	\bar{r}_{C-C}	1.462	1.431	1.227	1.433	1.453
		$\bar{r}_{C=C}$	1.436	1.494	-	1.358	1.478
		$\bar{r}_{C\equiv C}$	-	-	1.335	1.228	-
	MP2	\bar{r}_{C-C}	-	1.435	Unstable	1.436	-
		$\bar{r}_{C=C}$	-	1.483		1.366	-
		$\bar{r}_{C\equiv C}$	-	-		1.254	-
6-31G	MP2	\bar{r}_{C-C}	1.489	1.402	Unstable	1.357	TS
		$\bar{r}_{C=C}$	1.465	1.520		1.389	
		$\bar{r}_{C\equiv C}$	-	-		1.275	

3.2. Stability, Gap, Fermi and Atomization energies

Relative Stability

All four methods agree that the D_{6h} (Sheet) isomer has the lowest energy, ranking it in fact as the most stable. The Fig. 2 illustrates the relative energy histogram which reflects the chemical stability of the different isomers compared to the most stable one D_{6h} , as determined by the four methods. According to the calculations using the PBE-D3/cc-pVTZ, B3LYP/cc-pVTZ and B3LYP-D3/cc-pVTZ methods, the newly proposed D_{2d} structure is predicted to be stable. There is a significant difference in the relative stability of the D_{2d} structure between the PBE-D3/cc-pVTZ and B3LYP/cc-pVTZ methods, with a gap of approximately 13%. This difference can be solely attributed to the choice of the DFT functional, as the basis set remains the same for

both methods. Contrary to the observations regarding the geometry, when it comes to the relative stability predicted by B3LYP and B3LYP-D3 using the same basis set, both methods exhibit sometimes significant discrepancies depending on the isomer. For the D_{2d} and O_h isomers, the relative energy gap between the two methods is 0.03% and 3.3%, respectively. However, for D_{12h} and D_{6d} , this difference becomes much larger, attaining 64.9% and 70.5%, respectively. From this, we conclude that the dispersion effects, unlike the geometry case where they play a minor role, are crucial factors in determining the relative energies. However, it is worth noting that the D_{2d} structure is ranked last among the other structures. This observation could potentially be explained by its higher rigidity and stronger geometric constraints compared to the other geometric forms. However, most likely due to the use of the non-extended 6-31G basis set, the MP2 method predicts the D_{2d} structure to be a transition state.

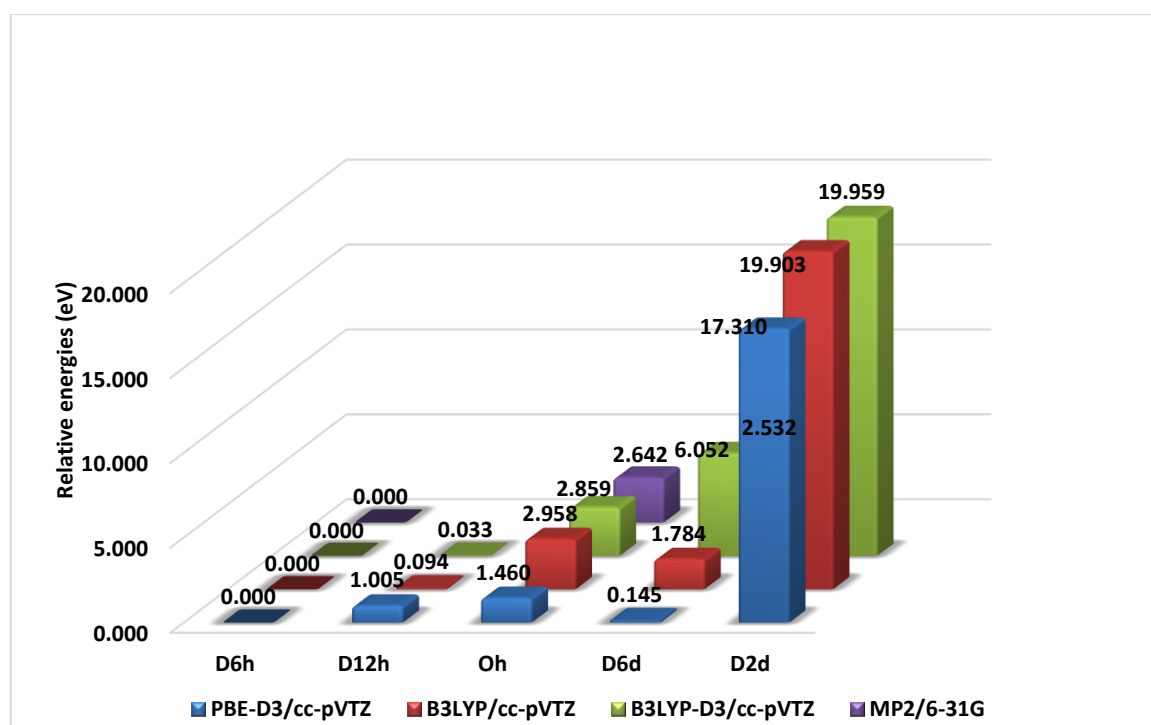


Fig. 2. Relative energies (eV) of the C_{24} isomers at PBE-D3/cc-pVTZ, B3LYP/cc-pVTZ, B3LYP-D3/cc-pVTZ and MP2/6-31G levels. *

* A violet cube, corresponding to MP/6-31G method, of height 2.532 exists, but is not visible, for the isomer D_{6d} .

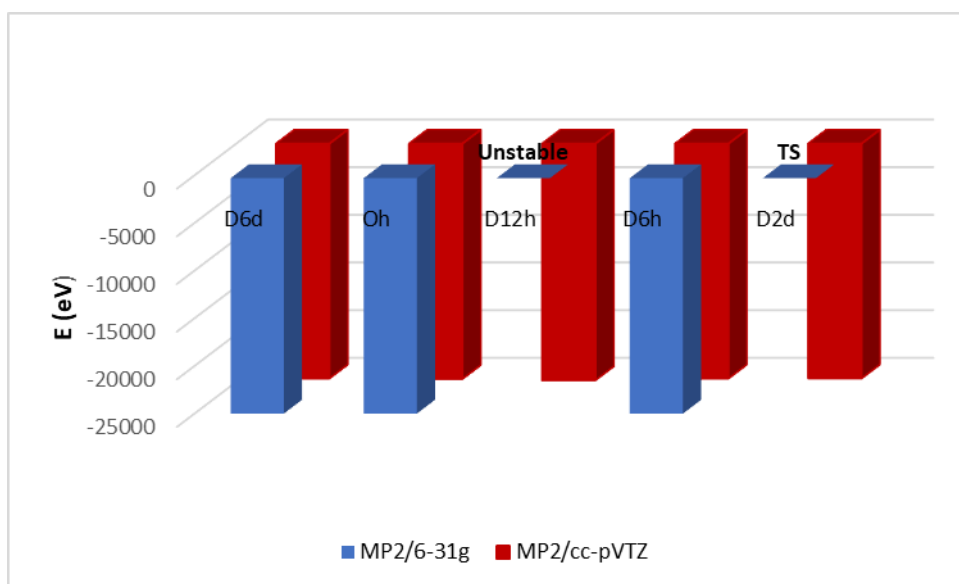


Fig. 3. Comparison in MP2 method between Optimized Energy calculations using the 6-31G for all five isomers, predicting D_{2d} to be TS and D_{12h} to be unstable, and those using the cc-pVTZ for three isomers (O_h, D_{12h} and D_{6h}). Also shown are the single point calculation of MP2/cc-pVTZ for the two isomers (D_{2d} and D_{6d}).

We illustrate in Fig. 3 a comparison, in the MP2 method, between the optimized energies using the basis set 6-31G for all isomers, where it predicts the isomer D_{2d} to be a transition state (TS) and D_{12h} to be unstable, and those using the basis set cc-pVTZ for the isomers (O_h, D_{12h}, D_{6h}), whereas we list also the single point calculation using the cc-pVTZ basis set in the two isomers (D_{2d} and D_{6d}) where convergence for optimization was not guaranteed. Actually, the figure reveals that while the MP2/6-31G optimization predicts an unstable D_{12h} isomer and a transition state for D_{2d}, the energy differences between the two methods are minimal for the other isomers. This implies and explains that significant energy changes can only occur after numerous iterations. Therefore, caution must be exercised when interpreting the results from a single MP2/cc-pVTZ calculation.

Atomization Energies

Table 7 and Figures 4 and 5 present the atomization energies (AE), Fermi energies (FE), and gap energies (GE) of the C₂₄ isomers obtained from calculations performed at four different levels of theory: (PBE-D3, B3LYP, B3LYP-D3)/cc-pVTZ, and MP2/6-31G for the five isomers, as well as MP2/cc-pVTZ for the two isomers O_h and D_{6h}. The atomization energies were determined using specific formulas:

$$AE = \frac{24 \cdot E_{Carbon} - E_{Molecule}}{24}$$

Table 7. Atomization energy (in eV/atom) of C₂₄ isomers at different calculations levels.

AE (eV/atom)						
Basis set	Method	D _{6d}	O _h	D _{12h}	D _{6h}	D _{2d}

cc-pVTZ	PBE-D3	8.729	8.670	8.690	8.340	8.010
	B3LYP	8.005	7.956	8.076	8.080	7.246
	B3LYP-D3	7.825	7.958	8.076	8.077	7.246
6-31G	MP2	6.200	6.196	Unstable	6.309	TS
cc-pVTZ		-	6.534	-	6.636	-
B3LYP/6-31+G* [25]		9.03	-	-	-	-

It is important to note that the MP2 method consistently yields lower atomization energy (AE) values compared to the PBE and B3LYP methods for each isomer. The average value of AE obtained from DFT-type methods (PBE-D3, B3LYP and B3LYP-D3) is 8.06 eV/atom, while the MP2 method with cc-pVTZ (6-31G) basis set provides an average value of 6,59 (6.24) eV/atom, which is approximately 23.6% lower than the DFT methods. Specifically, for the D_{6d} isomer, the average value of the AE using DFT methods (PBE-D3, B3LYP and B3LYP-D3) is 8.19 eV/atom, which is relatively close to the reference [25] calculated using the same method but through a different basis set, with a deviation of approximately 9.3%. Furthermore, it is worth noting that the PBE-D3 method consistently yields atomization energies AE that are higher than those obtained from the B3LYP and B3LYP-D3 methods by approximately 7.5%. Regarding the new D_{2d} structure, it is observed that its atomization energy AE in the PBE-D3 method deviates from the closest isomer, D_{6h} , by only 0.33 eV per atom. However, both the B3LYP and B3LYP-D3 methods distinctly separate the D_{2d} isomer from the D_{6d} isomer, exhibiting a noticeable deviation of 0.83 eV per atom for both methods.

Gap Energies

The gap energy (GE), is defined as the minimum amount of energy needed for an electron to move from the valence band to the conduction band, indicating whether the materials are conductors, semiconductors, or insulators. It is known [40], that a material is an insulator when the GE is larger than 3 eV, whereas it is a semi-conductor when the GE is moderately large between 0.1 to 3 eV, which is lower than in an insulator and is of the order of (~ 1 eV). For a conductor, conduction bands and valence bands are not separated and the GE is therefore vanishing.

Fig. 4 illustrates that the GE provided by the MP2 method (using cc-pVTZ and 6-31G basis set) is significantly larger than that of the PBE-D3, B3LYP and B3LYP-D3 methods. Furthermore, it is worth noting that both B3LYP and B3LYP-D3 methods produce almost identical GEs, but these gaps are 56.65% larger than those obtained from the PBE-D3 method. Specifically, the average DFT (PBE, B3LYP and B3LYP-D3) GE is 1.89 eV, whereas it is 7.63 (7.97) eV in the MP2/6-31G (/cc-pVTZ), representing an increase of approximately 75,7%. This substantial difference can be attributed to the use of the non-extended basis set in the MP2 method, which leads to that all C_{24} isomers behave as insulators. A similar trend is observed when comparing the two DFT methods, in that the average GE resulting from B3LYP and B3LYP-D3 methods is 2.33 eV, while the PBE-D3 method yields a value of 1.01 eV for the GE, representing an increase of 56.65%. The fact that the GE values of the B3LYP and the B3LYP-D3 methods are nearly identical suggests that the functional nature is likely the

determining factor in the discrepancy between (B3LYP + B3LYP-D3) on one side and PBE-D3 on the other side.

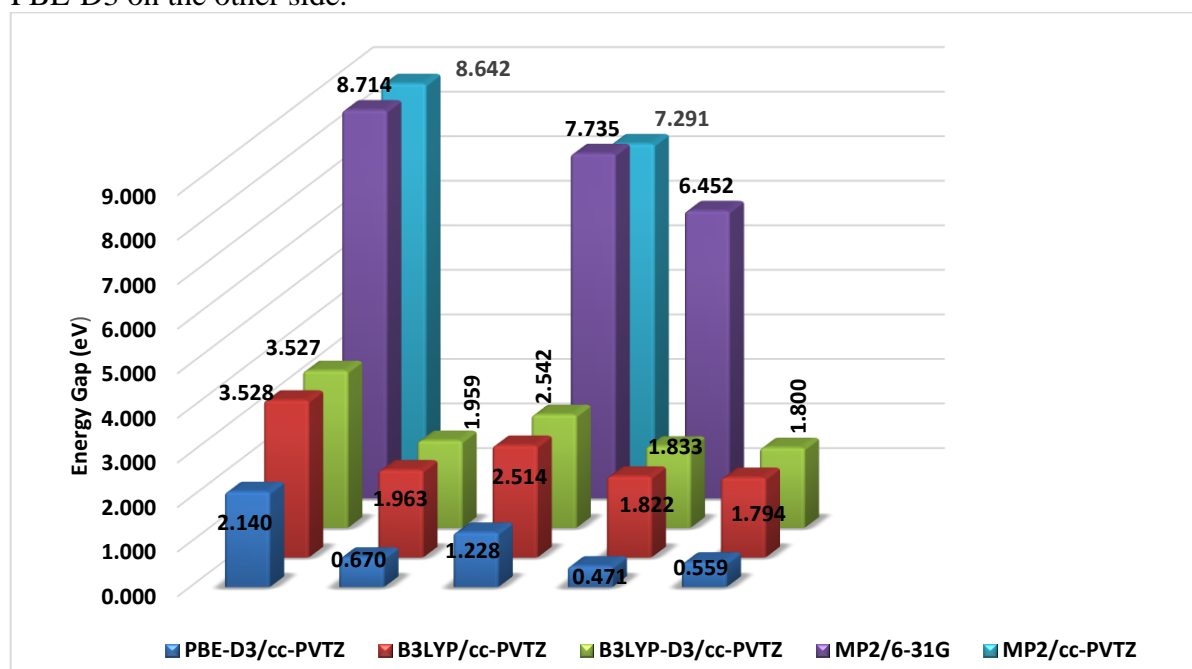


Fig. 4. The E_{Gap} energy (eV) of C₂₄ isomers (D_{6h}, D_{12h}, O_h, D_{6d} and D_{2d}, from left to right) at the PBE-D3, B3LYP, B3LYP-D3, MP2 (using both cc-pVTZ and 6-31G) levels.

The B3LYP-D3 method, as well as the B3LYP, notably overestimates the values of the GE compared to the lower values provided by PBE-D3. The average GE in the (B3LYP+B3LYP-D3) methods is approximately 2.32 eV, while it is 1.01 eV in the PBE-D3 method. Therefore, the (B3LYP+B3LYP-D3) methods yields GE values approximately 56.5% greater than those of PBE-D3. Both the PBE-D3 and (B3LYP+B3LYP-D3) methods agree that the D_{6h} isomer has the highest GE, despite having the lowest relative energy. The (B3LYP+B3LYP-D3) method establishes a correlation between the GE and the relative energy for the D_{2d} isomer, with the smallest GE in the (B3LYP+B3LYP-D3) method. However, this correlation is not maintained in the PBE method. We note that in all the methods used, the sheet isomer (D_{6h}) has the largest GE values compared to other isomers with the least electrical conductivity. According to the (B3LYP+B3LYP-D3) methods, the D_{2d} isomer has the smallest GE, while the PBE-D3 method predicts it to be D_{6d}. With the exception of the D_{6h} isomer which is to be considered a dielectric material with a GE of 3.53 eV and 2.14 eV in B3LYP and PBE respectively, the PBE and (B3LYP+B3LYP-D3) methods do not agree on the electrical conductivity of the C₂₄ isomers. Specifically, according to the PBE-D3 method, the D_{12h}, D_{6d}, D_{2d}, and O_h isomers are predicted to be semiconductors, while the (B3LYP+B3LYP-D3) methods classifies them as weak insulators. The MP2 method predicts a significantly clear insulating character for the D_{6h}, O_h, and D_{6d} isomers, making the D_{6h} isomer to be the most insulating among the five studied isomers. In comparison with other studies, we find an agreement when comparing with the previous theoretical calculations at B3LYP/6-31G (d) [27], giving

GE values of 1.825, 2.522, 1.881, and 3.425 eV for the D_{6d}, O_h, D_{12h}, and D_{6h} isomers respectively. On the other hand, when comparing our calculations at MP2 methods with previous theoretical calculations at the MP2/DZP level [20], where GE values of 7.346, 7.619, 8.435, and 9.251 eV were measured for the same isomers, respectively, we find also a good agreement. On the other hand, the results of the works [27], showed that the C₂₄ semiconducting fullerene isomers, except for the D_{6h} isomer, were also considered dielectric materials with a GE of 3.425 eV.

Fermi Energies

In Figure 5, we present the Fermi energy (FE) values of the five isomers calculated using the formula:

$$E_F = (E_{LUMO} + E_{HOMO})/2$$

using the four methods (PBE-D3, B3LYP, B3LYP-D3)/cc-pTVZ and MP2/6-31G, as well as those of the O_h and D_{6h} isomers using MP2/cc-pTVZ.

These FE values are shown according to the energy stability of the B3LYP/cc-pVTZ method from left to right (D_{6h}, D_{12h}, O_h, D_{6d} and D_{2d} respectively).

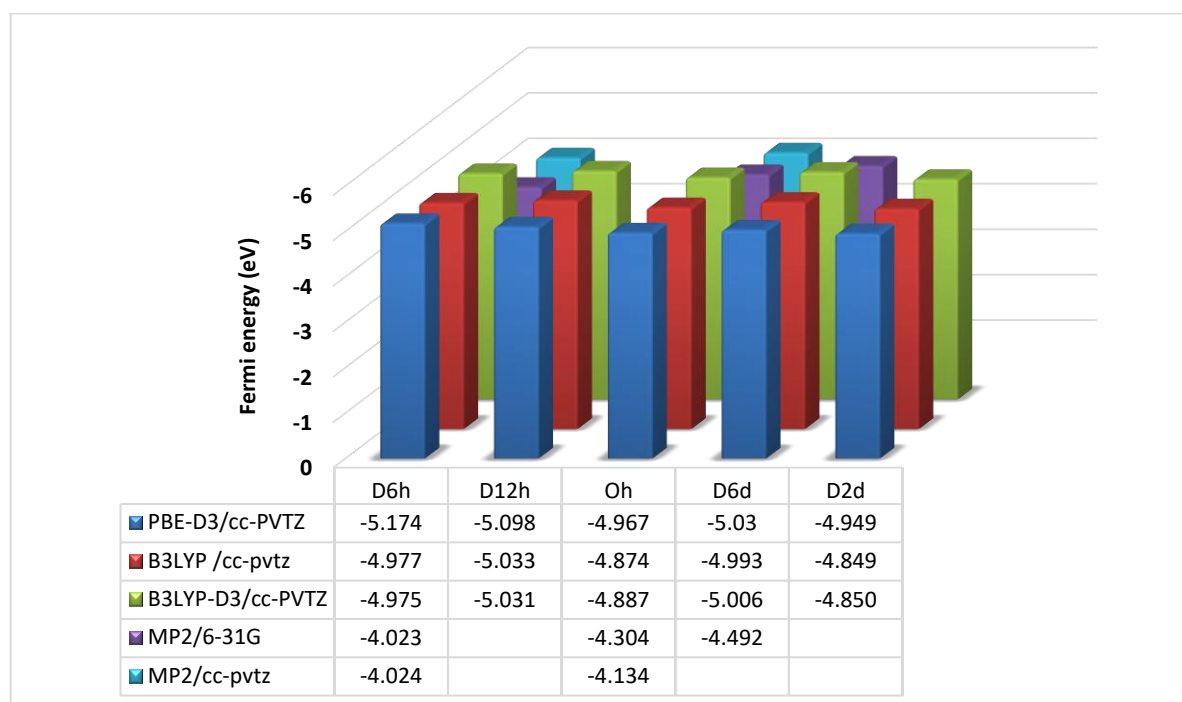


Fig. 5. Fermi energies (in eV) of the isomers of C₂₄ at PBE-D3, B3LYP, B3LYP-D3, MP2 (using cc-pVTZ) and MP2/6-31G levels.

Fig. 5 illustrates that the values of the FE for the five C₂₄ isomers calculated using the four methods are relatively comparable, exhibiting a contrasting behavior compared to the energy gap. From the figure 5, it is noticeable that the MP2 method consistently underestimates the FE values of the various stable isomers compared to the PBE-D3,

B3LYP and B3LYP-D3 methods. The average FE value predicted by the DFT methods (PBE-D3, B3LYP and B3LYP-D3) is 4.98 eV, whereas the MP2 method (using the two basis sets) provides a value of 4.20 eV, representing an increase of 15,7%. In contrast, the three DFT methods provide very similar values. The average FE value in the (B3LYP and B3LYP-D3) methods is 4.95, while in the PBE-D3 method it is 5.04, resulting in a 1.79% increase for PBE compared to (B3LYP and B3LYP-D3) methods. Additionally, both the PBE-D3 and (B3LYP and B3LYP-D3) methods agree that the D_{2d} isomer has the highest FE value, but they do not agree on ranking the isomer with the highest FE. The PBE-D3 method ranks the D_{6h} isomer as having the lowest FE, while (B3LYP and B3LYP-D3) assign this position to the D_{12h} isomer. The ranking of the isomer with the highest and lowest FE values by the PBE and (B3LYP and B3LYP-D3) methods is consistent with the ranking of the atomization energy discussed earlier. Moreover, we observe that the D_{6h} isomer has the highest FE at the MP2 level unlike the PBE-D3 and (B3LYP and B3LYP-D3) methods where it is the D_{2d} isomer which meets this property.

3.3. Electronic Properties of C₂₄ Isomers: Ionization Potential, Electronic Affinity, Hardness, and Electronegativity

The computed values of the ionization potential (IP), electronic affinity (EA), hardness (η), and electronegativity (χ) of all isomers are given in Tables (8 and 9). For the MP2 method, these values can be calculated from the HOMO and LUMO orbital energies using the following approximate expression:

$$IP = -E_{\text{Homo}} , \quad EA = -E_{\text{Lumo}}$$

$$\text{Electronegativity } (\chi) = \frac{(IP+EA)}{2}$$

$$\text{Hardness } (\eta) = \frac{(IP-EA)}{2}$$

The IP and EA values are determined using the PBE-D3 and (B3LYP and B3LYP-D3) methods with the cc-pVTZ basis set, employing the respective expressions:

$$IP = E(\text{optimized cation}) - E(\text{optimized neutral})$$

$$EA = E(\text{optimized neutral}) - E(\text{optimized anion})$$

Table 8. Ionization potential (IP) and electronic affinity (EA), in eV, of the C₂₄ isomers at (PBE-D3, B3LYP, B3LYP -D3, MP2)/cc-pVTZ and MP2/6-31G levels.

		IP (eV)				
Basis set	Method	D _{6d}	O _h	D _{12h}	D _{6h}	D _{2d}
cc-pVTZ	PBE-D3	7.219	7.571	6.973	8.096	7.190
	B3LYP	6.426	7.719	7.222	8.159	7.093
	B3LYP -D3	3.178	7.647	7.202	8.124	7.130
6-31G	MP2	7.718	8.172	Unstable	8.380	-

cc-pVTZ		-	7.780	-	8.345	-
6-31G(d)	B3LYP [26]	7.36	7.54	-	8.00	-
	B3LYP [41]	7.47	-	-	-	-
EA (eV)						
cc-pVTZ	PBE-D3	2.845	2.145	3.289	2.358	2.758
	B3LYP	2.474	2.110	2.936	1.911	2.609
	B3LYP -D3	6.813	2.058	2.869	1.939	2.584
6-31G	MP2	1.265	0.436	-	-0.333	-
cc-pVTZ		-	0.489	-	-0.296	-
6-31G(d)	B3LYP [41]	2.98	-	-	-	-
Exp. [42]		2.90	-	-	-	-

Table 9. Hardness (η) and electronegativity(χ), in eV, of the isomers of C_{24} at (PBE-D3, B3LYP, B3LYP-D3, MP2)/cc-pVTZ and MP2/6-31G levels.

η (eV)						
Basis set	Methods	D_{6d}	O_h	D_{12h}	D_{6h}	D_{2d}
cc-pVTZ	PBE-D3	2.187	2.713	1.842	2.869	2.216
	B3LYP	1.976	2.804	2.143	3.124	2.242
	B3LYP -D3	1.817	2.794	2.166	3.092	2.273
cc-pVTZ	MP2	-	3.645	-	4.320	-
6-31G		3.226	3.868	Unstable	4.356	TS
6-31G(d)	B3LYP[41]	0.89	-	-	-	-
χ (eV)						
cc-pVTZ	PBE-D3	5.032	4.858	5.131	5.227	4.974
	B3LYP	4.450	4.914	5.079	5.035	4.851
	B3LYP -D3	4.995	4.852	5.035	5.031	4.857
cc-pVTZ	MP2	-	4.134	Unstable	4.024	-
6-31G		4.491	4.304	-	4.023	-
6-31G(d)	B3LYP[41]	5.19	-	-	-	-

As shown in Tables 8 and 9, the IP, EA, η and χ values for all the five isomers were calculated using the DFT (PBE-D3, B3LYP, B3LYP-D3)/cc-pVTZ and the MP2/6-31G. In addition, the same values for the O_h and D_{6h} isomers using the MP2/cc-pVTZ level are stated.

The results indicate that, excluding the D_{6d} isomer at the B3LYP-D3 level, the IP values for the five isomers are similar among all four methods, consistent with a previous study [26] (and also [41]) which, using the B3LYP/6-31G(d) method, reported an average IP value of 7.42 eV, slightly lower than our average of 7.51 eV obtained through the DFT calculations. Furthermore, upon examining Table 8, several observations can be noted. For the isomers O_h , D_{12h} , D_{6h} , and D_{2d} , both the B3LYP and B3LYP-D3 methods yield almost identical IPs, which implies, for these isomers, that the dispersion correction has only a minor impact. In other words, the inclusion of the dispersion correction does not significantly alter the IP values obtained using the B3LYP method for these specific isomers.

Moreover, for all the isomers, the MP2 method (using 6-31G and cc-pVTZ basis sets) overestimates the IP values compared to those obtained from the DFT methods (B3LYP, B3LYP-D3, and PBE-D3). In simpler terms, the MP2 method, with its respective basis sets, tends to provide higher IP values for all isomers when compared to those obtained from the DFT methods (B3LYP, B3LYP-D3 and PBE-D3). Except for D_{6d}, the MP2 (6-31G and cc-pVTZ) method gives an average IP value of 8.17 eV, while DFT methods (B3LYP, B3LYP-D3, and PBE-D3) yield a lower average of 7.51 eV, showing an 8.1% decrease. For D_{6d} isomer, the MP2 (6-31G and cc-pVTZ) method gives an average IP of 7.39 eV, while the PBE-D3 and B3LYP methods yield 6.82 eV and the B3LYP-D3 gives 3.18 eV. The dispersion correction appears to have a significant impact on the IP value as it reduces the IP by 53.4%. The effect of expanding the basis set from 6-31G to cc-pVTZ on the MP2 calculations of the IP is minor for the D_{6h} isomer, whereas a substantial decrease is observed for the O_h isomer.

Putting aside the D_{6h}, the C₂₄ isomers exhibit positive EA values, indicating their ability to form stable anions. Among these isomers, D_{12h} shows the highest EA. Comparing the PBE-D3/cc-pVTZ and B3LYP/cc-pVTZ levels, the EA of D_{6d} is determined to be 2.845 eV and 2.474eV, respectively, which closely matches an experimental study reporting 2.90 eV [42], while a different theoretical approach using B3LYP/6-31G(d) yielded a slightly higher value of 2.98 eV [41]. Table 8 indicates that for the D_{6d} isomer, the EA provided by the PBE-D3 method is slightly higher than that provided by B3LYP. The average EA value for these two methods is 2.66 eV. However, the B3LYP-D3 method significantly overestimates the EA, giving a value of 6.81 eV, which represents a 60.9% increase compared to (PBE and B3LYP). Additionally, comparing the values provided by B3LYP and B3LYP-D3 suggests that dispersion terms lead to a 60.9% increase in the EA value, while for other isomers, their contribution is minor. Regarding the MP2 findings, it is evident that the MP2/6-31G method significantly underestimates the EA in comparison to the three DFT methods. This discrepancy is likely attributed to the constrained nature of the basis set employed, which might not fully capture the intricate electronic structure of the system. The results from Table 8 indicate that the PBE-D3 method slightly overestimates the EA values for the O_h, D_{12h}, D_{6h}, and D_{2d} isomers. Furthermore, the average EA obtained by the three DFT methods (PBE-D3, B3LYP, and B3LYP-D3) is 2.46 eV. Notably, the two MP2 methods (utilizing 6-31G and cc-pVTZ) yield very similar EA values. Specifically, the average EA for the O_h isomer is 0.46 eV, and for D_{6h}, it is -0.31 eV.

Hardness reflects a molecule's resistance to changes in electron distribution, with "hard" molecules, like D_{6d} with a large HOMO-LUMO gap, being less reactive. Conversely, softness suggests higher reactivity. Moreover, hardness indicates a molecule's ability to resist the deformation of its electron cloud during chemical processes.

According to Table 9, the three DFT methods (PBE-D3, B3LYP, and B3LYP-D3) yield hardness (η) and electronegativity (χ) values of comparable magnitude. The average values for each isomer and for the isomer series are as follows: (hardness; electronegativity) - (1.99; 4.83) for D_{6d}, (2.77; 4.61) for O_h, (2.05; 5.08) for D_{12h}, (3.03; 5.10) for D_{6h}, (2.24; 4.89) for D_{2d}, and (2.42; 4.90) for the isomer series.

On the other hand, the D_{6h} isomer demonstrates the highest hardness and electronegativity (χ) values at the PBE-D3, B3LYP, B3LYP-D3 and MP2 (utilizing cc-pVTZ and 6-31G) levels. Furthermore, the use of the MP2 method with cc-pVTZ and 6-31G leads to a significant overestimation of η . For the O_h and D_{6h} isomers, the MP2 method predicts η values of 3.65 eV and 4.32 eV, respectively, while the average η obtained from the DFT methods (PBE-D3, B3LYP, and B3LYP-D3) is 2.77 eV and 3.03 eV. This corresponds to an increase of 24% and 29.9%, respectively. Similar trends are observed when applying the MP2/6-31G method. In particular, for the D_{6d} isomer, the average η and χ obtained from the three DFT methods are 1.99 eV and 4.83 eV, respectively. However, other studies [41], which employed the B3LYP/6-31G(d) method, report significantly different values of 0.89 eV and 5.19 eV, resulting in discrepancies of 55.28% and 6.93%, respectively. In contrast, the MP2/6-31G method yields values of 3.23 eV and 4.49 eV, leading to deviations of 72.45% and 13.49%, respectively. These findings emphasize that despite having the same number of carbon atoms (24), the isomers differ in their molecular geometry, which accounts for the variation in their physical properties. Therefore, molecular geometry plays a vital role in determining the physicochemical properties of substances.

3.4. Electric Dipole Moment and Polarizabilities

Tables (10 and 11) present the results of electric dipole moment (μ) and static electric polarizability $\langle\alpha\rangle$ for the C_{24} isomers calculated at the PBE-D3, B3LYP, B3LYP-D3 and MP2, using the cc-pVTZ basis set and 6-31G basis set respectively.

Electric Dipole Moment

The electric dipole moment is a vector quantity that is significantly affected by the molecular symmetry and flexibility. It characterizes both the magnitude and direction of the electric charge separation within a molecule, and it is equal to the vector sum of the electric dipole moments of its individual bonds. When a molecule exhibits perfect symmetry in its structure and charge distribution, the individual bond moments cancel each other out, causing the overall dipole moment to vanish. However, as the molecule moves away from symmetry, the dipole moment increases, reflecting the growing charge separation within the molecule.

In Table (10) we show the dipole moment values calculated at the PBE-D3, B3LYP, B3LYP-D3, MP2 (utilizing cc-pVTZ) and the MP2/6-31G levels.

Table 10. Electric dipole moment (Debye) of the five C_{24} isomers at PBE-D3, B3LYP, B3LYP -D3, MP2 (using cc-pVTZ) and MP2/6-31G levels.

Dipole Moment (μ) $\times 10^{-4}$						
Basis set	Method	D_{6d}	O_h	D_{12h}	D_{6h}	D_{2d}
cc-pVTZ	PBE-D3	366.4	0.1	0.3	0.6	0.1
	B3LYP	11.5	0.1	6.2	0.2	0.1
	B3LYP -D3	7.6	0.1	6.8	0.2	0.1
6-31G	MP2	12.7	0.5	Unstable	0.0	TS

cc-pVTZ		-	0.0	-	0.0	-
6-311++ G(d,p)	B3LYP) [43]	0	-	-	-	-

According to Table 10, the dipole moment μ values for the D_{6d} isomer vary significantly among the four methods used in this study and the one utilized in an earlier work [43]. The differences in value range up to 97.9% when compared to our lowest value and to 100% compared to the B3LYP/6-311++G(d,p) result [43]. PBE-D3 seems to poorly represent μ compared to B3LYP and B3LYP-D3. However, the inclusion of dispersion terms in B3LYP-D3 lowers μ by 33.9% compared to B3LYP. The MP2/6-31G method provides a μ value that is 9.4% (40.2%) higher than that of B3LYP (B3LYP-D3). Considering the basis set extension used in [43], the value of 7.6 Debye (D) appears to be the most plausible among our results. Concerning the O_h isomer, the numerical complexity is reduced because all three DFT methods unexpectedly give the same μ value of 0.1 D, even though they use different functionals and account for dispersion in different ways. However, when employing the MP2/6-31G method, the dipole moment μ increases by 80% compared to the results obtained from the DFT methods.

In the case of the D_{12h} isomer, when incorporating dispersion terms in B3LYP, the dipole moment increases by 8.8% compared to the result obtained solely with the B3LYP method. The average dipole moment obtained from both B3LYP and B3LYP-D3 is 6.5 D, showing that it is 95.4% higher than the dipole moment obtained from the PBE-D3 method. In the case of D_{6h} , the situation is comparable in nature to D_{12h} . Adding dispersion terms to the B3LYP method does not have a notable impact on the results. The average dipole moment obtained from both B3LYP and B3LYP-D3 is 0.2 D due to its high symmetry, which is 66.7% lower than the dipole moment value obtained from the PBE method.

Lastly, we discuss the new D_{2d} bracelet isomer, where all three DFT methods yield identical μ values. The influence of functionals nature and dispersion terms seems to be negligible in this scenario. Furthermore, despite the diverse range of geometries observed among the isomers, the dipole moment remains constant during the transition from one isomer to another, which appears to be an unreasonable outcome. The conclusion drawn from this discussion regarding the dipole moment variation along the C_{24} isomer series reveals that despite the dipole moment being a first-order property, it is not straightforward to accurately replicate it. The selection of the functional and the approach employed to incorporate long-range interactions are determining factors in achieving accurate results. The three DFT methods indicate that D_{2d} and O_h isomers have equal and lowest dipole moments, whereas the B3LYP/6-311++G(d,p) [43] method suggests that D_{6d} occupies this position. It is evident that the three DFT methods (using cc-pVTZ) and MP2/6-31G concur that D_{6d} possesses the largest dipole moment in the isomer series, contrary to the previous study [43], which predicted D_{6d} to have the smallest dipole moment among all the isomers.

Atomic and Molecular static Polarizabilities

Table (11) presents the isotropic polarizability ($\langle\alpha\rangle$) of the stable C_{24} isomers calculated at the DFT (PBE-D3, B3LYP and B3LYP-D3) and MP2 levels using the cc-pVTZ basis set and 6-31G basis set respectively. The isotropic static electric polarizability $\langle\alpha\rangle$ is calculated as the mean value of those for the three molecule axes as expressed by:

$$\langle\alpha\rangle = \frac{\alpha_{xx} + \alpha_{yy} + \alpha_{zz}}{3}$$

Table 11. Comparison of the static electric polarizability values (evaluated in atomic units) for the C_{24} isomers at the (PBE-D3, B3LYP, B3LYP-D3)/cc-pVTZ and MP2/6-31G levels.

Molecular Polarizability (a.u)							Atomic Polarizability (a.u)	
Basis set	Method	D _{6d}	O _h	D _{12h}	D _{6h}	D _{2d}	α_c	$24*\alpha_c$
cc-pVTZ	PBE-D3	219.02	202.89	548.08	269.39	265.20	8.05	193.37
	B3LYP	201.23	198.85	498.59	259.19	259.40	7.91	189.92
	B3LYP -D3	201.92	199.40	498.26	259.01	260.52	7.91	189.92
6-31G	MP2	189.33	172.57	Unstable	223.27	TS	5.07	121.82
6-31+G(d)	B3LYP [44]	215	-	-	-	-	-	-
6-311+G(d)	PBEPBE [45]	187.13	-	-	-	-	-	-
6-311++G(d,p)	B3LYP [43]	216.19	-	-	-	-	-	-
Atomic Polarizability (a.u) (Previous work)								
Comments		α_c		Ref.				
NR, CASPT2, ML res.		11.39		[46]				
NR, CCSD(T), ML res.		11.67±0.07						
R, Dirac+Gaunt,CCSD(T)		11.26±0.20						
recommended		11.3±0.2						

Regarding the atomic electric polarizability $\langle\alpha_c\rangle$, the three DFT methods yield highly similar results, with an average value of 7.96 atomic units (a.u.), representing a reduction of approximately 29.5% compared to the recommended value in [45]. This is noteworthy considering the utilization of an expanded basis set and a reliable functional. In contrast, the MP2/6-31G method shows a larger deviation, exhibiting a difference of 55.1% from the recommended value.

Concerning molecular polarizabilities, the predicted MP2 values are of the same order of magnitude, but are smaller compared with the DFT methods. According to Table 11, the PBE-D3 method consistently gives higher molecular polarizabilities than B3LYP, B3LYP-D3, and MP2 methods. Specifically, for the D_{6d} isomer, both B3LYP and B3LYP-D3 produce very similar polarizabilities, averaging at 201.58 a.u., which is 7.9% lower than the PBE-D3 result. The dispersion correction in B3LYP only contributes minimally to the differences observed. On the other hand, the MP2/6-31G method yields a polarizability 6.1% smaller than the average of B3LYP and B3LYP-D3, and 13.6% smaller than PBE-D3. Interestingly, our MP2/6-31G polarizability is only 1.2% different from the one obtained in a previous study [45] using PBE/6-311+G(d). Moreover, an earlier research [43-44] reports an average polarizability of

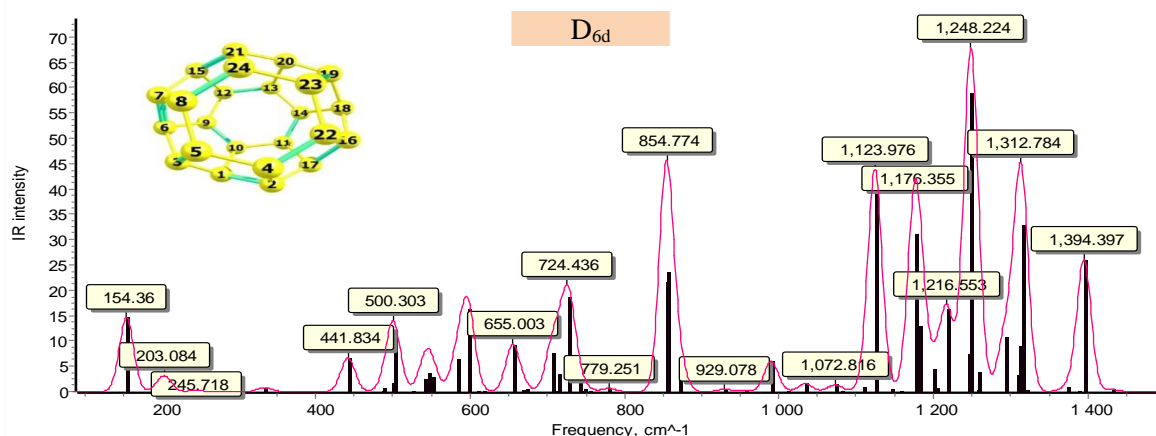
215.60 a.u. obtained with the B3LYP method using 6-31+G(d) and 6-311++G(d,p) basis sets, showing an increase of 6.5% compared to the average of our B3LYP and B3LYP-D3 calculations with the cc-pVTZ basis set, and a 12.2% increase compared to our MP2/6-31G value. Regarding the O_h isomer, the inclusion of dispersion corrections in the B3LYP method has a noticeable but relatively minor effect. The average polarizability calculated using B3LYP and B3LYP-D3 is 199.12, which is 1.86% lower than the polarizability obtained from PBE-D3. On the other hand, the MP2/6-31G method yields a polarizability that is 14.94% smaller than the PBE-D3 value and 13.3% smaller than the average polarizability obtained from the combination of B3LYP and B3LYP-D3. For the D_{12h} isomer, we see a comparable trend to the previous isomer, where the inclusion of dispersion correction in B3LYP has minimal effect, resulting in B3LYP-D3 values closely resembling those of B3LYP. The average polarizability obtained from B3LYP and B3LYP-D3 is 498.43 a.u., indicating a decrease of 9.1% compared to the polarizability obtained from PBE-D3. In a similar manner, the D_{6h} isomer's polarizability is highly similar for both the B3LYP and B3LYP-D3 methods due to the negligible impact of dispersion corrections. The average polarizability from these two methods is 259.1, representing a decrease of 3.8% compared to the polarizability obtained from PBE-D3. However, the MP2/6-31G method shows a polarizability that is 17.1% smaller than the PBE-D3 value and 13.8% smaller than the polarizability obtained from B3LYP and B3LYP-D3. Similar to O_h , the D_{2d} isomer follows the same trend. The inclusion of dispersion correction in B3LYP has a small, yet significant, impact. The average polarizability obtained from B3LYP and B3LYP-D3 is 259.96, indicating a decrease of 1.98% compared to the polarizability obtained from PBE-D3. PBE-D3 and B3LYP-D3 methods exhibiting a consistent agreement regarding the ranking of polarizabilities in ascending order, with the exception of D_{6h} and D_{2d} isomers, which are ranked oppositely between the two methods. All the methods unanimously determine that O_h (D_{12h}) possesses the smallest (highest) polarizability. Considering the minimal differences between the polarizabilities obtained from B3LYP and B3LYP-D3, we investigated the variations in polarizability within the isomer series when comparing PBE to the average of B3LYP and B3LYP-D3, noted as "Mean (B3LYP, B3LYP-D3)". The results, in ascending order, are 3.77 for O_h , 5.24 for D_{2d} , 10.29 for D_{6h} , 17.45 for D_{6d} , and 49.66 for D_{12h} . However, when comparing PBE to MP2, the polarizability differences are 29.69 for D_{6d} , 30.32 for O_h , and 46.12 for D_{6h} . There is no consistent correlation observed between the rankings of the smallest and largest differences in polarizability between PBE- Mean (B3LYP, B3LYP-D3) and PBE-MP2. It is worth noting that the polarizability of D_{12h} is highly influenced by the choice of the DFT method, as it becomes similar to D_{6h} when comparing DFT methods. Conversely, O_h is the isomer that exhibits weak dependence on the DFT method, but it becomes comparable to D_{6d} and shares similarities with it.

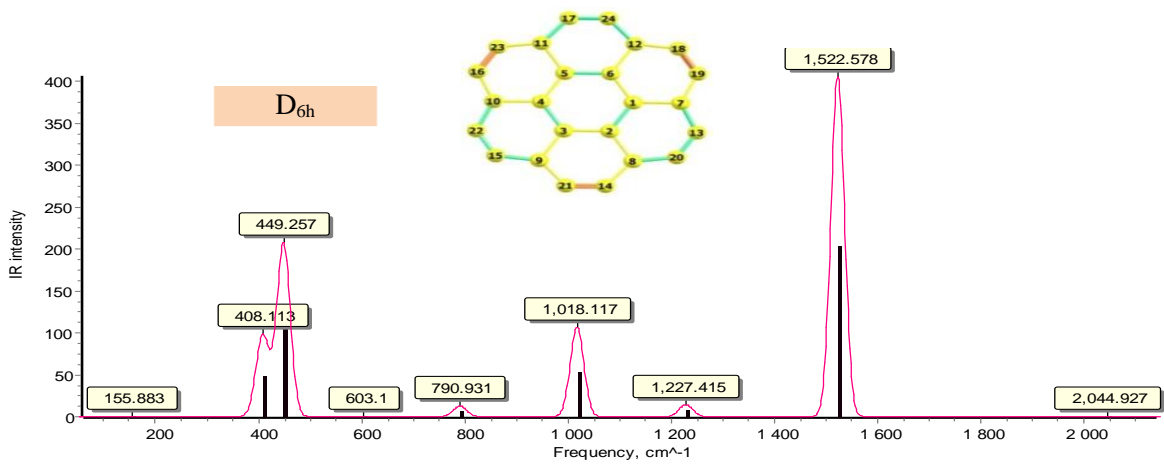
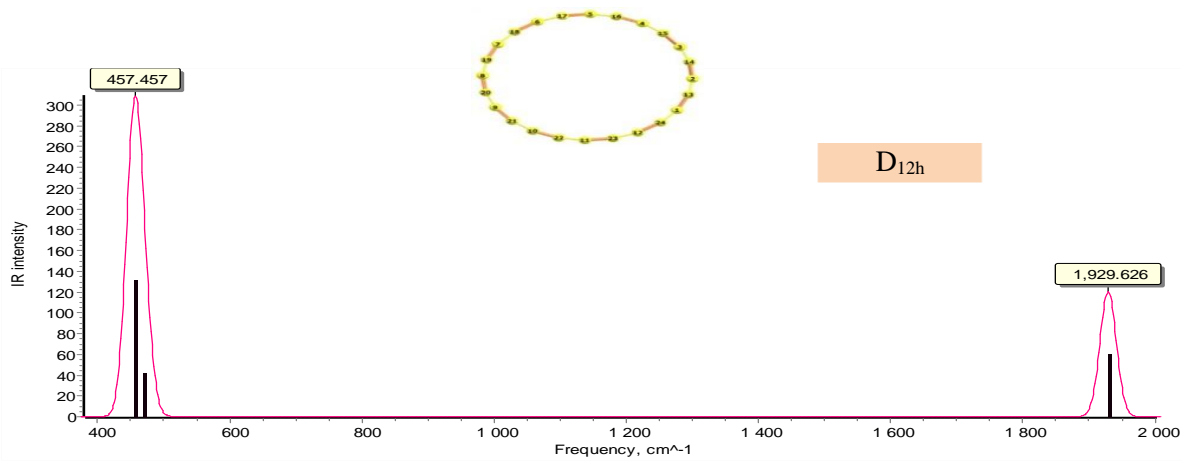
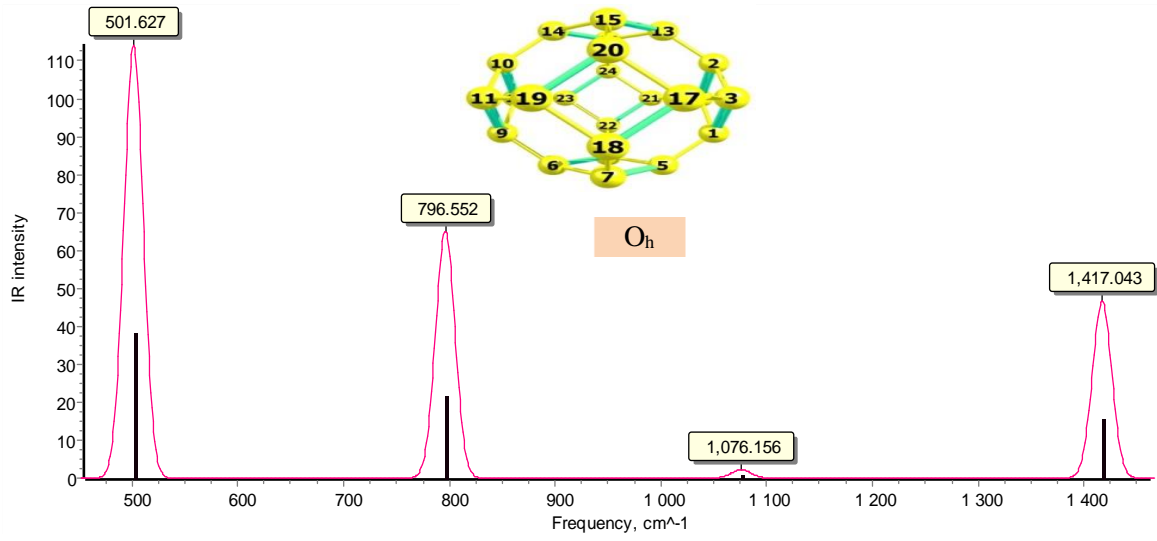
When comparing the sum of atomic Polarizabilities with the molecular polarizability, the two values are found to be comparable in the O_h isomer when calculated within the MP2 framework. For the other isomers, the additive sum of atomic Polarizabilities differs much from the molecular value. Finally, compared to other more sophisticated methods, the predicted MP2 and DFT atomic polarizability values of carbon atom are significantly underestimated.

To summarize, as polarizability is a second-order property, it is highly sensitive to the molecular geometry and to the choice of wavefunction or functional used in calculations, as evident from its comparison with the electric dipole moment. The impact of dispersion terms is relatively minor in the B3LYP method, but it becomes more substantial in the PBE method. However, quantitatively assessing the individual contributions of the functional and dispersion corrections for PBE remains a challenging task.

3.5. Vibration Frequencies and Infrared Spectra

The C_{24} isomers has a total of 66 vibrational modes ($3N-6$, where N is the number of atoms). Figure 5 displays the vibrational frequencies and infrared (IR) spectra of C_{24} isomers at the PBE-D3 level of theory using the cc-pVTZ basis set. The results of B3LYP/cc-pVTZ, B3LYP-D3/cc-pVTZ and MP2/6-31G are reported in Figures S1 and S2 of the supplementary materials file. These figures visually represent the data and illustrate the variations in vibrational frequencies and IR spectra among the different isomers. The isomer with the highest symmetry, the ring isomer, exhibits the fewest peaks (2) in its spectrum. The O_h isomer, with lower symmetry, has 3 peaks, followed by the Bracelet D_{2d} isomer with 4 peaks, followed by the sheet D_{6h} with 5 peaks, and finally the D_{6d} with 13 peaks, according to the three DFT methods. Furthermore, the absorption wavelengths obtained from DFT calculations are quite comparable to those from MP2 calculations. The influence of electronic correlation and dispersion effects becomes evident when comparing the wavelengths originating from the MP2 calculation with those from the and PBE one. The way by which the electronic correlation is taken into account, as well as the consideration of non-covalent interactions, becomes evident when comparing the absorption wavelengths obtained from the PBE, B3LYP, B3LYP-D3 and MP2 methods.





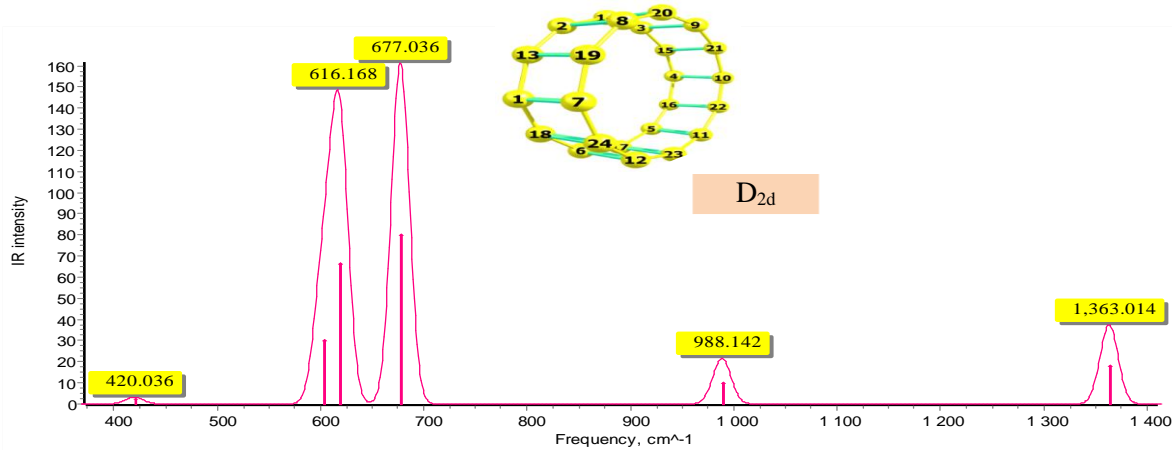
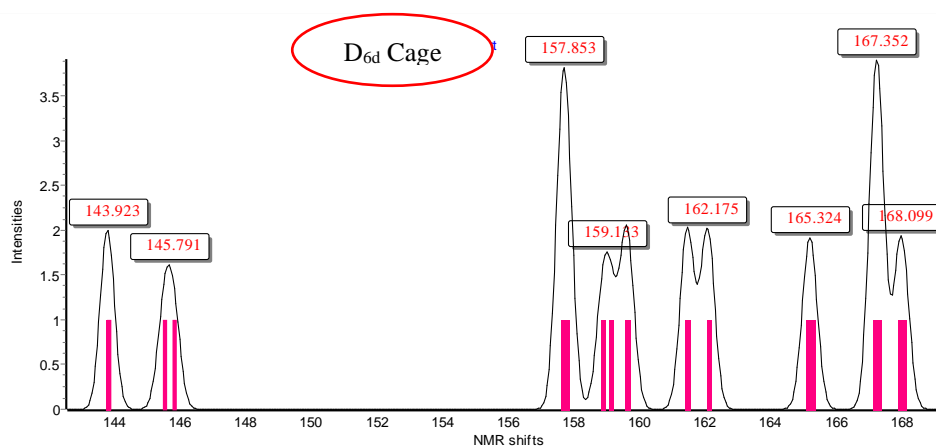


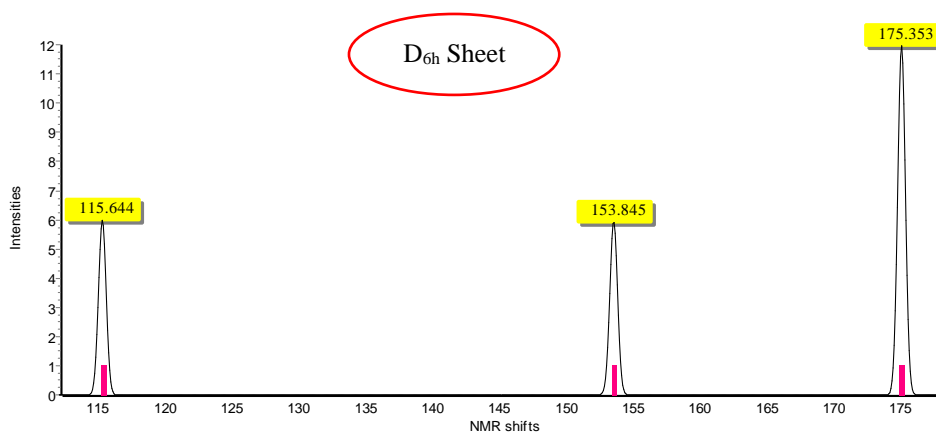
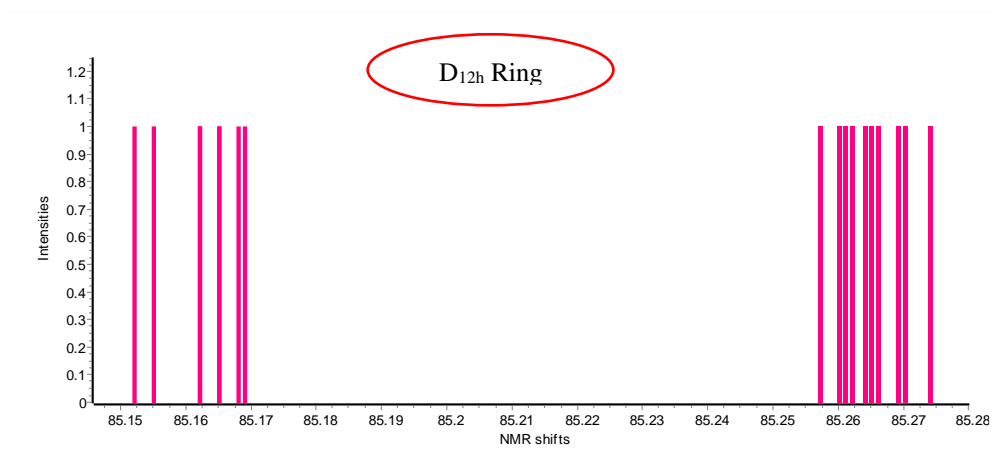
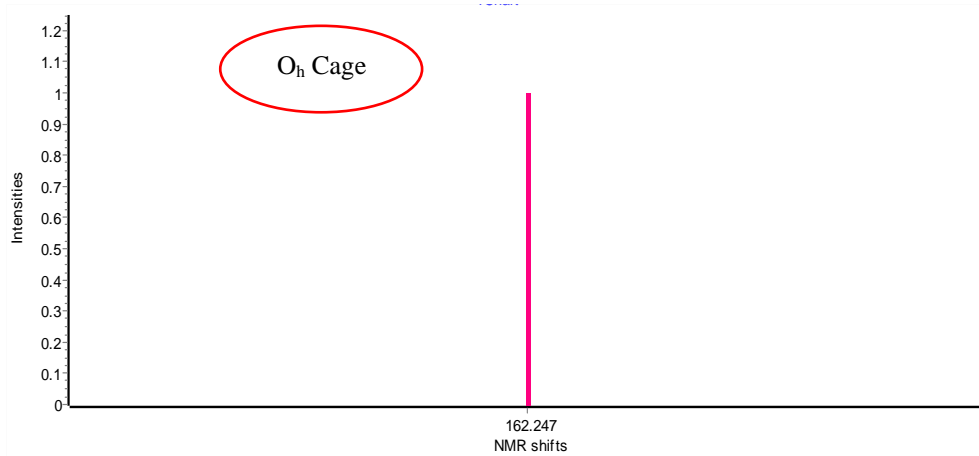
Fig. 6. Infrared spectra of the C_{24} isomers at PBE-D3/cc-PVTZ level.

3.6. NMR Spectra for the C_{24} isomers

We report in Tables S3, S4, S5, S6, S7, and S8 placed in the supplementary material file, the values (in ppm) of the isotropic and anisotropic nuclear screening constants (σ) of the C_{24} isomers calculated at the PBE, B3LYP, B3LYP-D3 levels of theory using the cc-pVTZ basis set.

These tables show that, for the D_{6d} isomer, the average (σ) of atoms belonging to the pentagonal shape is equal to 20.772 ppm, whereas this average value is 54.121 ppm for atoms in the hexagonal ring. These different values allow us to distinguish clearly between the two types of atoms. For the O_h and D_{12h} isomers, all carbon atoms are quasi-equivalent and have a mean isotropic (σ) part of about 30.431 ppm. For the D_{6h} isomer, the value of (σ) is distributed in three classes. First, the mean value of (σ) for the central hexagonal cycle (atoms C_1 - C_6) is about 29.784 ppm. Second, for peripheral atoms, linked to the central hexagonal cycle (C_7 - C_{12}), the mean value of (σ) is 67.948 ppm. Third, this average mean increases to 99.067 ppm for peripheral atoms, not linked to the central hexagonal cycle (C_{13} - C_{24}), which indicates that the electron density on these atoms is higher, leading to a shielding effect. For the D_{2d} isomer, the value of (σ) is distributed in two classes. First, the mean value of (σ) (atoms $C_3, C_6, C_9, C_{12}, C_{13}, C_{16}, C_{19}$, and C_{22}) is about 29.784 ppm. Second, for peripheral atoms, linked to the central hexagonal cycle (C_7 - C_{12}), the mean value of (σ) is 67.948 ppm. As for the remaining atoms, the mean value of (σ) is 59.882 ppm.





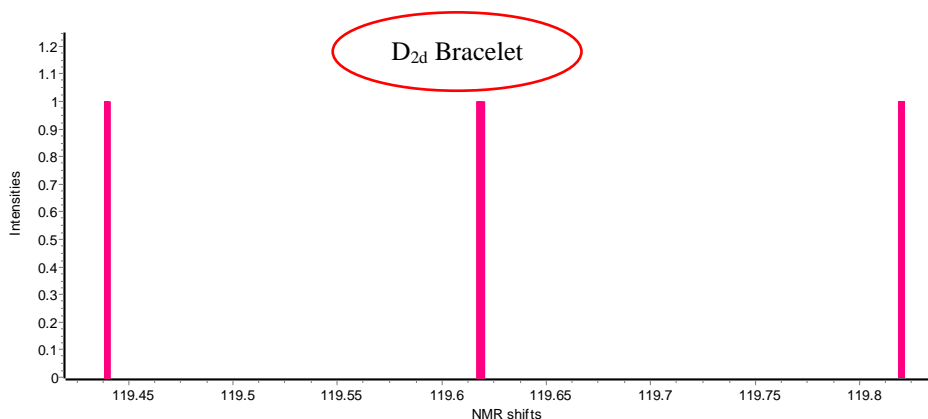


Fig. 7. NMR spectra of the C_{24} isomers at PBE-D3/cc-pVTZ level.

5. Conclusion

In this study, we investigated multiple aspects of C_{24} isomers (D_{6d} , O_h , D_{12h} , D_{6h} , and D_{2d}) using the PBE-D3, B3LYP, B3LYP-D3 (cc-pVTZ) and MP2/6-31G methods. We analyzed geometry optimizations, relative stability, static electric polarizabilities, nuclear screening constants, gap and atomization energies, thermodynamic analysis, vibration frequencies, as well as infrared and NMR spectra.

Consistently, the D_{6h} isomer was found to be the most stable among the studied C_{24} isomers, while the newly proposed D_{2d} isomer exhibited the least stability. The B3LYP and B3LYP-D3 methods consistently predicted higher energy gap (GE) values compared to PBE, with an average DFT (PBE, B3LYP and B3LYP-D3) GE of 1.89 eV. In contrast, the MP2 method indicated a significantly higher GE value of 7.63 eV, representing a substantial increase of approximately 75%. Regarding the electronic character, PBE classified the D_{12h} , D_{6d} , D_{2d} , and O_h isomers as semiconductors, whereas B3LYP or B3LYP-D3 classified them as weak insulators. On the other hand, the MP2 method predicted a distinct insulating character for the D_{6h} , O_h , and D_{6d} isomers, with the D_{6h} isomer being the most insulating among the studied isomers. The PBE-D3 method consistently provides higher polarizabilities of the C_{24} isomers compared to B3LYP, B3LYP-D3 and MP2 methods. This underscores the significance of considering electronic correlation and dispersion effects for accurate prediction of polarizabilities.

The results obtained from different methods emphasize the impact of methodology on the predicted properties, highlighting the need for careful analysis and interpretation of theoretical results for diverse geometries. Notably, the study reveals that O_h has the smallest polarizability, and D_{12h} exhibits the highest polarizability, indicating a significant influence of the applied electric field on its electronic cloud, a consensus among all methods. Moreover, the polarizability of D_{12h} significantly depends on the chosen DFT method, while O_h shows less sensitivity but shares similarities with D_{6d} . Additionally, the D_{12h} isomer displayed the highest number of

absorption peaks, while the calculated nuclear screening constants allowed for distinguishing the magnetically equivalent carbon atom groups in each isomer.

In conclusion, our study provides valuable insights into the stability, electronic properties, and polarization behavior of C₂₄ isomers. The findings underscore the importance of methodology selection and electronic correlation and dispersion considerations in accurately predicting properties and interpreting theoretical results for the C₂₄ isomers with varying geometries.

Data Availability Statement

Not applicable.

Declaration of competing interest

The authors report no conflicts of interest. The authors alone are responsible for the content and writing of this article.

Acknowledgments

N. Chamoun acknowledges support from the PIFI-CAS program, from Humboldt Foundation, and from ICTP Associate program.

Supporting Information Available: Are reported as supplemental information: Cartesian coordinates of C₂₄-D_{2d} isomer optimized at the PBE-D3/cc-pVTZ level of theory, optimized energies and thermodynamic analysis using the four methods PBE, B3LYP, B3LYP-D3 and MP2, nuclear screening constants using PBE, B3LYP and B3LYP-D3 and IR spectra paragraphs using MP2, B3LYP and B3LYP-D3. This material is available free of charge via the Internet at:

References

- [1] Kroto, H. W., Allaf, A. W., & Balm, S. P. (1991). C₆₀: Buckminsterfullerene. *Chemical Reviews*, 91(6), 1213-1235. <https://doi.org/10.1021/cr00006a005>.
- [2] Kazemzadeh, H., & Mozafari, M. (2019). Fullerene-based delivery systems. *Drug Discovery Today*, 24(3), 898-905. <https://doi.org/10.1016/j.drudis.2019.01.013>
- [3] Parasuk, V., & Almlöf, J. (1991). C₂₀: the smallest fullerene?. *Chemical Physics letters*, 184(1-3), 187-190. [https://doi.org/10.1016/0009-2614\(91\)87185-E](https://doi.org/10.1016/0009-2614(91)87185-E).
- [4] Noël, Y., De La Pierre, M., Zicovich-Wilson, C. M., Orlando, R., & Dovesi, R. (2014). Structural, electronic and energetic properties of giant icosahedral fullerenes up to C₆₀₀₀: insights from an ab initio hybrid DFT study. *Physical Chemistry Chemical Physics*, 16(26), 13390-13401. DOI: 10.1039/c4cp01442a.
- [5] Kroto, H. W., Heath, J. R., O'Brien, S. C., Curl, R. F., & Smalley, R. E. (1985). C₆₀: Buckminsterfullerene. *nature*, 318(6042), 162-163. <https://doi.org/10.1038/318162a0>

- [6] Kroto, H. W. (1987). The stability of the fullerenes C_n , With $n=24, 28, 32, 36, 50, 60,$ and 70 . *Nature*, 329, p529. <https://doi.org/10.1038/329529a0>
- [7] Feyereisen, M., Gutowski, M., Simons, J., & Almlöf, J. (1992). Relative stabilities of fullerene, cumulene, and polyacetylene structures for C_n : $n=18-60$. *The Journal of chemical physics*, 96(4), 2926-2932. <https://doi.org/10.1063/1.461989>
- [8] T. Guo, M. D., Diener, Y., Chai, A. J., Alford, R. E., Haufler, S. M., & McClure, T. & et al. (1992). Uranium Stabilization of C_{28} - A Tetravalent Fullerene. *Science*, 257(5077), 1661-1664. <https://doi.org/10.1126/science.257.5077.1661>.
- [9] Raghavachari, K., Zhang, B., Pople, J. A., Johnson, B. G., & Gill, P. M. W. (1994). Isomers of C_{24} . Density functional studies including gradient corrections. *Chemical physics letters*, 220(6), 385-390. [https://doi.org/10.1016/0009-2614\(94\)00192-8](https://doi.org/10.1016/0009-2614(94)00192-8).
- [10] Jones, R. O., & Seifert, G. (1997). Structure and bonding in carbon clusters C_{14} to C_{24} : chains, rings, bowls, plates, and cages. *Physical review letters*, 79(3), 443.
- [11] Piskoti, C., Yarger, J., & Zettle, A. (1998). C_{36} , a new carbon solid. *Nature*, 393, pp: 771-4. <https://doi.org/10.1103/PHYSREVLETT.79.443>.
- [12] Paulus, B. (2003). Electronic and structural properties of the cage-like molecules C_{20} to C_{36} . *Physical Chemistry Chemical Physics*, 5(16), 3364-3367. DOI: 10.1039/b304539k.
- [13] Chang, Y. F., Zhang, J. P., Sun, H., Hong, B., An, Z., & Wang, R. S. (2005). Geometry and stability of fullerene cages: C_{24} to C_{70} . *International journal of quantum chemistry*, 105(2), 142-147. <https://doi.org/10.1002/qua.20691>.
- [14] An, W., Shao, N., Bulusu, S., & Zeng, X. C. (2008). Ab initio calculation of carbon clusters. II. Relative stabilities of fullerene and non-fullerene C_{24} . *The Journal of chemical physics*, 128(8), 084301. <https://doi.org/10.1063/1.2831917>.
- [15] Pattanayak, J., Kar, T., & Scheiner, S. (2004). Substitution Patterns in Mono BN-Fullerenes: C_n ($n = 20, 24, 28, 32, 36$ and 40). *J. Phys. Chem. A.*, 108, P 7681. <https://doi.org/10.1021/jp047833m>.
- [16] Talanov, V. M., Fedorova, N. V., & Gusarov, V. V. (2010). Symmetrical Features of the Structure of C_{24} and C_{48} Fullerenes. *Glass Physics and Chemistry*, 36(3), 358-368. DOI: 10.1134/S1087659610030132.
- [17] Von Helden, G. V., Hsu, M. T., Gotts, N. G., Kemper, P. R., & Bowers, M. T. (1993). Do small fullerenes exist only on the computer? Experimental results on C_{-20} and C_{+24} . *Chemical physics letters*, 204(1-2), 15-22. [https://doi.org/10.1016/0009-2614\(93\)85599-J](https://doi.org/10.1016/0009-2614(93)85599-J).
- [18] Kent, P. R. C., Towler, M. D., Needs, R. J., & Rajagopal, G. (2000). Carbon clusters near the crossover to fullerene stability. *Physical Review B*, 62(23), 15394.
- [19] Martin, J. M., El-Yazal, J., & François, J. P. (1996). On the structure and vibrational frequencies of C_{24} . *Chemical physics Letters*, 255(1-3), 7-14. [https://doi.org/10.1016/0009-2614\(96\)00347-8](https://doi.org/10.1016/0009-2614(96)00347-8).
- [20] Jensen, F., & Toftlund, H. (1993). Structure and stability of C_{24} and $B_{12}N_{12}$ isomers. *Chemical physics letters*, 201(1-4), 89-96. [https://doi.org/10.1016/0009-2614\(93\)85039-Q](https://doi.org/10.1016/0009-2614(93)85039-Q).
- [21] Jensen, F., & Koch, H. (1998). C_{24} : Ring or fullerene?. *The Journal of chemical physics*, 108(8), 3213-3217. <https://doi.org/10.1063/1.475716>.

- [22] Balevišius, L. M., Stumbrys, E., & Tamulis, A. (1997). Conformations and electronic structure of fullerene C₂₄ and C₂₆ molecules. *Fullerenes, Nanotubes, and Carbon Nanostructures*, 5(1), 85-96. <https://doi.org/10.1080/15363839708011974>.
- [23] Stewart, J. J. (1990). MOPAC manual. Constraints, 3(2).
- [24] Popov, A. P., & Bazhin, I. V. (2007). Cubic polymerized structures of small fullerenes C₂₀, C₂₄, C₂₈, C₃₂. In *Hydrogen Materials Science and Chemistry of Carbon Nanomaterials* (pp. 713-719). Springer, Dordrecht. https://doi.org/10.1007/978-1-4020-5514-0_89.
- [25] Anafche, M., and F. Naderi. "A Comparative DFT Study on Structural and Electronic Properties of C₂₄ and Some of Its Derivatives: C₁₂B₆N₆, B₆N₆C₁₂ and B₁₂N₁₂." (2012): 329-335.
- [26] Manna, D., & Martin, J. M. (2016). What are the ground state structures of C₂₀ and C₂₄? An explicitly correlated ab initio approach. *The Journal of Physical Chemistry A*, 120(1), 153-160. <https://doi.org/10.1021/acs.jpca.5b10266>.
- [27] Wang, Z., Zhang, J., & Cao, Z. (2010). Theoretical studies on electronic structures and thermal stabilities of C₂₄O isomers derived from C₂₄. *Journal of Molecular Structure: THEOCHEM*, 949(1-3), 88-90. <https://doi.org/10.1016/j.theochem.2010.03.009>.
- [28] Sadjadi, S., Kwok, S., Cataldo, F., García-Hernández, D. A., & Manchado, A. (2020). A theoretical investigation of the possible detection of C₂₄ in space. *Fullerenes, Nanotubes and Carbon Nanostructures*, 28(8), 637-641. <https://doi.org/10.1080/1536383X.2020.1731735>.
- [29] Kaur, M., Sawhney, R. S., & Engles, D. (2013, July). To evince pure C₂₄ as superconducting mechanically controllable break junction configuration. In *International Conference on Advanced Nanomaterials & Emerging Engineering Technologies* (pp. 426-430). IEEE. DOI: [10.1109/ICANMEET.2013.6609336](https://doi.org/10.1109/ICANMEET.2013.6609336).
- [30] Zhao, W. K., Yang, C. L., Zhao, J. F., Wang, M. S., & Ma, X. G. (2012). Orientation effect on the electronic transport properties of C₂₄ fullerene molecule. *Physica B: Condensed Matter*, 407(12), 2247-2253. <https://doi.org/10.1016/j.physb.2012.03.008>.
- [31] Zhang, Y., & Cheng, X. (2018). Hydrogen storage property of alkali and alkaline-earth metal atoms decorated C₂₄ fullerene: A DFT study. *Chemical Physics*, 505, 26-33. <https://doi.org/10.1016/j.chemphys.2018.03.010>.
- [32] Ahangari, M. G., & Mashhadzadeh, A. H. (2020). Density functional theory based molecular dynamics study on hydrogen storage capacity of C₂₄, B₁₂N₁₂, Al₁₂N₁₂, Be₁₂O₁₂, Mg₁₂O₁₂, and Zn₁₂O₁₂ nanocages. *International Journal of Hydrogen Energy*, 45(11), 6745-6756. <https://doi.org/10.1016/j.ijhydene.2019.12.106>.
- [33] Sathe, R. Y., Bae, H., Lee, H., & Kumar, T. D. (2020). Hydrogen storage capacity of low-lying isomer of C₂₄ functionalized with Ti. *International Journal of Hydrogen Energy*, 45(16), 9936-9945. <https://doi.org/10.1016/j.ijhydene.2020.02.016>.
- [34] Mahamiya, V., Shukla, A., & Chakra borty, B. (2022). Exploring yttrium doped C₂₄ fullerene as a high-capacity reversible hydrogen storage material: DFT investigations. *Journal of Alloys and Compounds*, 897, 162797. <https://doi.org/10.1016/j.jallcom.2021.162797>.
- [35] Mahamiya, V., Shukla, A., & Chakra borty, B. (2022). Scandium decorated C₂₄ fullerene as high-capacity reversible hydrogen storage material: insights from density functional theory

- simulations. *Applied Surface Science*, 573, 151389. <https://doi.org/10.1016/j.apsusc.2021.151389>.
- [36] J Zhang, M Dolg - *Physical Chemistry Chemical Physics*, 2015 - pubs.rsc.org
Zhang, J., & Dolg, M. (2015). ABCluster: the artificial bee colony algorithm for cluster global optimization. *Physical Chemistry Chemical Physics*, 17(37), 24173-24181.
- [37] Neese, F. (2022). Software update: The ORCA program system—Version 5.0. *Wiley Interdisciplinary Reviews: Computational Molecular Science*, 12(5), e1606. <https://doi.org/10.1002/wcms.1606>.
- [38] Andrienko, G. A. *Chemcraft. Graphical Software for Visualization of Quantum Chemistry Computations*, 2010. Google Scholar There is no corresponding record for this reference.
- [39] Pokropivny, V. V., & Ivanovskii, A. L. (2008). New nanoforms of carbon and boron nitride. *Russian Chemical Reviews*, 77(10), 837. DOI: [10.1070/RC2008v077n10ABEH003789](https://doi.org/10.1070/RC2008v077n10ABEH003789).
- [40] Üngördü, A., & Tezer, N. (2017). The solvent (water) and metal effects on HOMO-LUMO gaps of guanine base pair: A computational study, *J. Mol Graph Model*, 74, 265–72. <https://doi.org/10.1016/j.jmgm.2017.04.015>.
- [41] Heidari Nezhad Janjanpour, M., Vakili, M., Daneshmehr, S., Jalalierad, K., & Alipour, F. (2018). Study of the ionization potential, electron affinity and HOMO-LUMO gaps in the small fullerene nanostructures. *Chemical Review and Letters*, 1(2), 45-48.
- [42] S. Yang, K. I. Taylor, M. I. Craycraft, I. Conceico, C. I. Pettiette, O. Cheshnovsky, and R. E. Smalley, *Chern. Phys. Lett.* 144,431 (1988).
- [43] Soyarslan, K., Ortatepe, B., Yurduguzel, B., Güllüoğlu, M. T., & Erdogdu, Y. U. S. U. F. (2022). An investigation into the structural, electronic, and non-linear optical properties in CN (N= 20, 24, 26, 28, 30, 32, 34, 36, and 38) fullerene cages. *Journal of Molecular Modeling*, 28(11), 352.
- [44] Kosar, N., Tahir, H., Ayub, K., & Mahmoud, T. (2021). DFT studies of single and multiple alkali metals doped C24 fullerene for electronics and nonlinear optical applications. *Journal of Molecular Graphics and Modelling*, 105, 107867. <https://doi.org/10.1016/j.jmgm.2021.107867>.
- [45] Omid, M., Sabzehzari, M., & Shamlouei, H. R. (2020). Influence of super alkali oxides on structural, electrical and optical properties of C24 fullerene nanocluster: A theoretical study. *Chinese Journal of Physics*, 65, 567-578. <https://doi.org/10.1016/j.cjph.2020.02.032>.
- [46] Schwerdtfeger, P., & Nagle, K. J. (2019). Table of Static Dipole Polarizabilities of the Neutral Elements in the Periodic Table (vol 117, pg 1200, 2018). *Mol. Phys*, 117, 1585. <https://doi.org/10.1080/00268976.2018.1535143>.